Phylogenomic insights into the divergent history and hybridization within the East Asian endemic *Abelia* (Caprifoliaceae)

Qing-Hui Sun[1], Diego F. Morales-Briones[2], Hong-Xin Wang[1], Jacob B. Landis[3,4], Jun Wen[5], Hua-Feng Wang[1]*

[1] *Key Laboratory of Tropical Biological Resources of Ministry of Education, College of Tropical Crops, Hainan University, Haikou 570228, China*

[2] *Department of Plant and Microbial Biology, College of Biological Sciences, University of Minnesota, 140 Gortner Laboratory, 1479 Gortner Avenue, Saint Paul, MN 55108, USA*

[3] *School of Integrative Plant Science, Section of Plant Biology and the L.H. Bailey Hortorium, Cornell University, Ithaca, NY 14850, USA*

[4] *BTI Computational Biology Center, Boyce Thompson Institute, Ithaca, NY 14853, USA*

[5] *Department of Botany, National Museum of Natural History, MRC-166, Smithsonian Institution, PO Box 37012, Washington, DC 20013-7012, USA*

*Authors for correspondence:

Hua-Feng Wang, E-mail: hfwang@hainanu.edu.cn

Abstract:

- **Background and Aims** *Abelia* (Caprifoliaceae) is a small genus with five species (including one artificial hybrid). The genus has a disjunct distribution across mainland China, Taiwan and the Ryukyu Islands, providing a model system to explore species dispersal mechanisms of the East Asian flora. However, the current phylogenetic relationships within *Abelia* remain controversial.
- **Methods** In this study, we reconstructed the phylogenetic relationships within *Abelia* using nuclear loci generated by target enrichment and the cpDNA from genome skimming.
- **Key Results** We found large cytonuclear discordance across the genus. Based on the nuclear and chloroplast phylogenies we proposed to merge *A. schumannii* into *A. macrotera*, and *A. macrotera* var. *mairei* into *A. uniflora*. Divergence time estimation, ancestral area reconstruction, and ecological niche modelling (ENM) were used to examine the biogeographic history of *Abelia*. Our results showed that *Abelia* originated in Southwest China, and diversification began in the Early Eocene, followed by *A. chinensis* var. *ionandra* colonizing Taiwan in the Middle Miocene. The ENM results suggested an expansion of climatically suitable areas during the Last Glacial Maximum and range contraction during the Last Interglacial. Disjunction between the Himalaya-Hengduan Mountain region (HHM) and Taiwan is most likely the consequence of topographic isolation and postglacial contraction.
- **Conclusions** Overall, our results supports that postglacial range contraction together with topographic heterogeneity resulted in the Taiwan and China mainland disjunction. Furthermore, when we using genome data to reconstruct the phylogeny of related species, branch evolution and network evolution should be considered, as well as gene flow in historical periods. This research provide new insights for the speciation process and taxonomy of *Abelia*.

Key words: *Abelia*; Phylogeography; Divergence time; Ancestral distribution; Taiwan

INTRODUCTION

The underlying causes of disjunct distributions in various organisms have been a central issue in biogeography (e.g., Xiang et al., 1998; Wen, 2001; Qian and Ricklefs, 2004; Wang et al., 2012; Wen et al., 2013, 2019). Much discussion has focused on two mechanisms: vicariance and long-distance dispersal (Doyle et al., 2004; Givnish and Renner, 2004; Yoder and Nowak, 2006; Šarhanová et al., 2017; Wang et al., 2020). The emergence of geographic barriers has led to vicariance, resulting in decreased gene flow; while long-distance dispersal in plants usually involves rare events driven by dispersal vectors such as animals, wind or water currents (Nathan et al., 2008). Recent molecular systematic studies have shown that many plant disjunctions are too young to be explained by continental drift or major geographic barriers (Doyle et al., 2004; Mummenhoff et al., 2004; Yoder and Nowak, 2006; Linder et al., 2013; Thomas et al., 2014, 2017; Jiang et al., 2019). Hence, long-distance dispersal has emerged as a major mechanism to explain many discontinuous distributions in historical geography (Wen et al., 2013; Ye et al., 2019; Wen and Wagner, 2020).

Biogeographic disjunctions between mainland China and Taiwan have received considerable attention with the separation of the two regions by 130 km (Wu and Wang, 2001; Xiang and Soltis, 2001; Qiu et al., 2011; Chen et al., 2012; Ye et al., 2014). Taiwan is the largest subtropical mountainous island in the monsoonal western Pacific region, located on the Tropic of Cancer and originating in the late Miocene (ca. 9-5 million years ago; Sibuet and Hsu, 2004). Molecular phylogenetic analyses have shown that several plant lineages have disjunct distributions between mainland China and Taiwan (e.g., *Sassafras* J. Presl, Nie et al., 2007; *Pseudotsuga* Carrière, Wei et al., 2010; *Triplostegia* Wall. ex DC., Niu et al., 2018). Geologically, Taiwan and its adjacent continental margin of China belong to the Eurasian plate; in the Late Cretaceous both of these were part of the continental block. The continental block has undergone many extensions and rifting events since the Paleocene (Zhang, 1995; Suo et al., 2015). Two hypotheses have been proposed to explain the formation of current plant disjunctions in this region: long-distance dispersal and postglacial contraction (Chou et

al., 2011; Wang et al., 2013; Ye et al., 2014; Niu et al., 2018). A phylogeographic study of *Cunninghamia* R.Br. ex A.Rich. (Taxodiaceae) revealed that populations in Taiwan were derived from continental Asia via long-distance seed dispersal (Lu et al., 2001). Factors that have had major impacts on population dynamics and genetic variation patterns in plants include past geological and climatic changes, uplift of the Qinghai-Tibet Plateau, global optimum temperature since the Miocene and the Quaternary glacial-interglacial transition (Xu et al., 2015; Cao et al., 2016; Chen et al., 2020). Recent studies have suggested that although the ice sheet was not ubiquitous from the Qinling Mountains and Huai River (at ca. 34° N) to the tropical south (≤ 22° N) in China during the Last Glacial period, the temperature in most parts of mainland China was lower than today (Shi et al., 2006). Temperature changes influence species distribution, population sizes, and intraspecific genetic differentiation. The postglacial contraction hypothesis states that many species had a continuous distribution from mainland China to Taiwan during the Quaternary glacial period, sometimes with disjunctions between the Himalaya-Hengduan Mountain region and Taiwan occurring when taxa migrated to higher altitudes as global temperatures increased (Chen and Ying, 2012).

Abelia R.Br. belongs to the subfamily Linnaeoideae Raf. within Caprifoliaceae s.l. (Dipsacales; Yang and Landrein, 2011; Caprifoliaceae; Wang et al., 2021). The genus includes *A. chinensis* (four varieties), *A. forrestii* (two varieties), *A. schumannii*, *A. macrotera* (eight varieties) and *A. uniflora* (Landrein et al., 2017; 2020; Fig. 1). *Abelia* is a typical East Asian endemic genus with a disjunct distribution between mainland China and Taiwan, mainly distributed in southwestern China, extending to eastern Taiwan and the Ryukyu Islands of Japan. The genus includes an important ornamental species, *Abelia* × *grandiflora*, widely cultivated in the yards, parks and roadsides of temperate cities (e.g., Beijing, London, Wuhan and Washington D.C; Fig. 1). However, the phylogenetic relationships within *Abelia* remain controversial due to limited markers and sampling, and hence the biogeographic history and process of speciation are still unclear. Kim (1998) used one nuclear (ITS) and one plastid (*matK*) marker to infer the phylogenetic relationships within *Abelia*. However, species

relationships could not be clarified because only two *Abelia* species were included, and a polytomy existed between the two *Abelia* species and those of *Diabeia*. Three *Abelia* species were included (*A. chinensis*, *A. schumannii* and *A. engleriana*) in Jacobs et al. (2010), but no information about relationships can be inferred since the three formed a polytomy. Using ITS and nine plastid regions (*rbcL*, *trnS-G*, *matK*, *trnL-F*, *ndhA*, *trnD-psbM*, *petB-D*, *trnL-rpl32* and *trnH-psbA*), Wang et al. (2015) found that *A. forrestii* was sister to all other *Abelia* species, while *A. chinensis* was sister to *A.* × *grandiflora* with moderate support. Although Landrein (2017) included 46 accessions of *Abelia* (22 natural taxa and 24 horticultural breeds), using only ITS and three plastid (*rbcL*, *trnL-F* and *matK*) genes, the species phylogeny was still unclear due to lack of resolution and low to moderate bootstrap support for many nodes.

Chloroplast DNA inheritance is primarily from the maternal parent in most angiosperms, therefore it cannot resolve the entire phylogenetic history of lineages (Corriveau and Coleman, 1988; Birky, 1995; Xue et al., 2020). Target enrichment has shown to be an effective approach to extract orthologous nuclear genes and can infer the phylogenetic relationships of complex taxa successfully (e.g., *Helianthus* L., Stephens et al., 2015. Asteraceae Bercht and J. Presl, 2018; *Pinus taeda* L., Neves et al., 2013; Caprifoliaceae, Wang et al., 2021). Therefore, we have chosen this approach for conducting a phylogenetic and biogeographic study of *Abelia*. In this study, using a target enrichment dataset we aim to (1) clarify the species-level phylogeny of *Abelia* based on nuclear genes and plastome data; and (2) reconstruct the biogeographic history of *Abelia* and explore its distribution patterns related to the disjunction between mainland China and Taiwan.

MATERIALS AND METHODS

Sampling, genomic data generation

We sampled 38 individuals from all five species of *Abelia* (Landrein, 2017; 2020) and several potential hybrid individuals, including *A.* × *grandiflora.* Six Linnaeoideae species

[*Diabelia serrata*, *D. sanguinea*, *Kolkwitzia amabilis*, *Dipelta floribunda* (two individuals), *Linnaea borealis*, and *Vesalea occidentails*] were used as outgroups. Voucher specimens were deposited in the herbarium of the Institute of Tropical Agriculture and Forestry of Hainan University (HUTB), Haikou, China. The complete list of taxa and information of data sources are provided in TableS1.

DNA was extracted from dried leaf tissue using a modified cetyltrimethylammonium bromide (CTAB) method, with chloroform: isoamyl alcohol separation and isopropanol precipitation at -20□ (Doyle and Doyle, 1987). We checked the concentration of each extraction with a Qubit 2.0 Fluorometer (Thermo Fisher Scientific, Waltham, MA, USA) and sonicated 400□ng of DNA using a Covaris S2 (Covaris, Woburn, MA) to produce fragments ~150 - 350□bp in length for making sequencing libraries. To ensure that genomic DNA was sheared to the appropriate fragment size, we evaluated all samples on a 1.2% (w/v) agarose gel.

We used a Hyb-Seq approach (Weitemier et al., 2014), which combines target enrichment and genome skimming. In our analysis, we obtained nuclear data from target enrichment and the cpDNA from genome skimming. We used the method to targeted 428 putatively single-copy orthologous genes using baits designed across Dipsacales (Wang et al., 2021). Hybridization, enrichment and sequencing methods followed those of Wang et al. (2021). Detailed descriptions of plastome sequencing methods can be found in Wang et al. (2020a).

Read processing and assembly

Raw reads were cleaned using Trimmomatic v.0.36 (Bolger et al., 2014) by removing adaptor sequences and low-quality bases (ILLUMINACLIP: TruSeq_ADAPTER: 2:30:10 SLIDINGWINDOW: 4:5 LEADING: 5 TRAILING: 5 MINLEN: 25). Nuclear loci were assembled with HybPiper v.1.3.1 (Johnson et al., 2016). Exon assemblies were carried out individually to avoid chimeric sequences in multi-exon genes produced by potential paralogy

(Morales-Briones et al., 2018) and only exons with a reference length of more than 150 bp were assembled.

Paralog detection was performed for all exons with the 'paralog_investigator' warning. To obtain 'monophyletic outgroup'(MO) orthologs (Yang and Smith, 2014), all assembled loci (with and without paralogs detected) were processed following Morales-Briones et al (2020).

For plastome assembly, raw reads were trimmed using SOAPfilter_v2.2. Adapter sequences and low-quality reads with Q-value ≤ 20 were removed. Clean reads were assembling against the plastomes of *Kolkwitzia amabilis*(KT966716.1) (Bai et al., 2017) using MITObim v.1.8 (Hahn et al., 2013). Assembled plastomes were also preliminarily annotated with Geneious R11.04 (Biomatters Ltd., Auckland, New Zealand) to detect possible inversions/rearrangements, with corrections for start/stop codons based on published *Abelia* plastomes(*A. chinensis*, Accession No. MN384463.1; *A. forrestii*, Accession No. MN524636.1; *A. macrotera*, Accession No. MN524637.1; *A.* × *grandiflora*, Accession No. MN524635.1). Detailed descriptions of plastome assembly methods can be found in Wang et al. (2020a).

Phylogenetic analyses

Nuclear dataset. We analyzed the nuclear data set using concatenation and coalescent-based methods. Individual exons were aligned with MAFFT and aligned columns with more than 90% missing data were removed using Phyutility prior to concatenation. Maximum likelihood (ML) analysis was conducted using RAxML v.8.2.20 (Stamatakis, 2014) with a partition-by-locus scheme and using the GTRGAMMA nucleotide substitution model for all partitions (Table 2). Clade support was assessed with 100 rapid bootstrap replicates. Additionally, we used Quartet Sampling (QS; Pease et al., 2018) to distinguish strong conflict from weakly supported branches. We carried out QS with 1000 replicates. We used ASTRAL-III v.5.7.1 (Zhang et al., 2018) for species tree estimation. We used RAxML with a GTRGAMMA model to generate individual exon trees as input. Local posterior probabilities (LPP) were used to calculate branch support (Sayyari and Mirarab, 2016).

Plastome dataset. Complete plastomes were aligned with MAFFT v.7.407 (Katoh and Standley, 2013) and aligned columns with more than 90% missing data were removed using Phyutility (Smith and Dunn, 2008). We performed extended model selection (Kalyaanamoorthy et al., 2017) followed by ML gene tree inference and 200 non-parametric bootstrap replicates for branch support in IQ-TREE v.1.6.1 (Nguyen et al., 2015). Additionally, we evaluated branch support with QS using 1,000 replicates.

Species network analysis

Morphological transitions were observed among several species during our field investigations and contradictory topologies were also obtained in our phylogenetic analyses. Due to computational restrictions and given our primary focus on potential reticulation between different species, we reduced the 45-taxon data set to one outgroup and 14 ingroup taxa representing all major clades based on the nuclear analyses. We looked for evidence of hybridization (reticulation) within *Abelia* via species network search carried out with the InferNetwork_MPL function in PhyloNet (Wen et al., 2018). Network searches were carried out using only nodes in the gene trees that had at least 50 percent bootstrap support, enabling up to five hybridization events and optimizing the branch lengths and probabilities of inheritance of the returned species networks under the full probability. To disentangle nested hybridization, we also created a reduced, 12-taxa data set by removing three hybrid taxa (*A.*× *grandiflora* E159, *A.*× *grandiflora* E227 and *A.*× *grandiflora* E226; see results) and carried out analyses previously described. We used the command 'CalGTProb' in PHYLONET to calculate the probability scores of the concatenated RAxML, ASTRAL, and plastid DNA trees, given the individual gene trees, to estimate the optimal number of hybridizations and measure if the species network matched our gene trees better than a purely bifurcating species tree.Finally, we selected the model using the bias-corrected Akaike information criterion (AICc; Sugiura, 1978), Akaike information criterion (AIC; Akaike, 1973), and the Bayesian information criterion (BIC; Schwarz, 1978). The network with the lowest AICc, AIC and BIC scores were selected as the best-fit-species network.

Divergence time estimation

To examine the historical biogeography of *Abelia*, we performed a dated phylogenetic analysis using BEAST v.1.8 (Drummond et al., 2012). As there is potential ancient hybridization in *Abelia*, we estimated diversification dates separately using the nuclear and the cpDNA data. We selected the fruit fossil of *Diplodipelta* from the late Eocene Florissant flora of Colorado (34.07 Ma; Manchester and Donoghue, 1995; Manchester, 2000; Bell and Donoghue, 2005) to calibrate the node containing *Diabelia* and *Dipelt*a, as the fossil shows morphological similarities to the two genera. We set a lognormal prior for the divergence at the stem of *Diabelia* and its sister clade *Dipelta* (offset 36 Ma, log-normal prior distribution 34.07-37.20 Ma). The ancestral node of Dipsacales (the root of our tree) was constrained to 50.18 Ma (mean 50.18 Ma) despite the lack of fossil evidence from results of previous studies in the literature(e.g., Li et al., 2019; Wang et al., 2021). The BEAST analyses were performed using an uncorrelated log-normal (UCLN) relaxed clock with a Yule tree prior, random starting trees, and GTR + G as model of sequence evolution (as selected by MrModelTest). For the BEAST analyses involving the prior, both nuclear and chloroplast data sets were used. Each MCMC run was conducted for 100,000,000 generations and sampling every 5,000 generations. The first 10 % of trees were discarded as burn-in. We used Tracer v.1.6 to assess convergence and effective sample size (ESS) > 200 (Rambaut et al., 2014). Tree Annotator v.1.8.0 (Drummond et al., 2012) was used to summarize the set of post-burn-in trees and their parameters in order to produce a maximum clade credibility chronogram showing the mean divergence time estimates with 95% highest posterior density (HPD) intervals. FigTree v.1.4.2 (Drummond et al., 2012) was used to visualize the resulting divergence times.

Ancestral area reconstructions

We examined the historical biogeography of *Abelia* using the Bayesian binary MCMC (BBM) analysis implemented in RASP v.3.21 (Yu et al., 2015). To account for phylogenetic

uncertainty, 5,000 out of 20,000 post-burn-in trees from the BEAST analyses (cpDN data) were randomly chosen for the BBM analyses. We compiled distribution data for the species of *Abelia* and assigned the included taxa to their respective ranges. Considering the areas of endemism in *Abelia* and tectonic history of the continent, we used three areas: (A) Southwest China, (B) Central-East China, and (C) Taiwan. Each sample was assigned to its respective area according to its contemporary distribution range (Table S1). We set the root distribution to null, applied 10 MCMC chains each run for 100 million generations, sampling every 10,000 generations using the JC + G model. The MCMC samples were examined in Tracer v.1.6 (Drummond et al., 2012) to confirm sampling adequacy and convergence of the chains to a stationary distribution. Tree Annotator v.1.8.0 (Drummond et al., 2012) was used to summarize the set of post-burn-in trees and their parameters in order to produce a maximum clade credibility chronogram showing the mean divergence time estimates with 95% highest posterior density (HPD) intervals.

Ecological niche modelling

We performed Ecological Niche Modelling (ENM) on *Abelia* using MAXENT v.3.2.1(Phillips et al., 2006). For the input we obtained 200 species occurrence data from the Chinese Virtual Herbarium (CVH, https://www.cvh.ac.cn/), Global Biodiversity Information Facility (http://www.gbif.org/) and personal observations. The details of these occurrence data are listed in Table S2. We used 19 bioclimatic variables as environmental data for ENM representing five different time periods. Past and current data for these variables were available from the WorldClim database (http://worldclim.org/). The data included baseline climate (BioClim layers for the period 1950-2000 at a spatial resolution of 30 s arc), data for the last glacial maximum (LGM; ~22 000 years BP) with spatial resolution at 2.5 min arc resolution simulated by Community Climate System Model (CCSM model), Max Planck Institute Model (MPI model) and Model for Interdisciplinary Research on Climate (MIROC model), and the last interglacial period. Replicate runs (25) of MAXENT were performed to ensure reliable results. Model performance was assessed using the area under the curve (AUC)

of the receiver operating characteristic. AUC scores may range between 0.5 (randomness) and 1 (exact match), with those above 0.9 indicating good performance of the model (Swets, 1988). The MAXENT jackknife analysis was used to evaluate the relative importance of the 19 bioclimatic variables employed. All ENM predictions were visualized in ArcGIS v.10.2 (ESRI, Redlands, CA, USA).

Analysis of character evolution

Four morphological characters (the number of epicalyx bracts, the number of flowers, inflorescence, corolla shape) of *Abelia* were used to reconstruct the evolution of morphological features. The character states were encoded according to Landrein (2017) and Landrein et al. (2020). The number of epicalyx bracts were scored with the following: (0) Four epicalyx; (1) Six epicalyx. The number of flowers were scored with the following: (0) Flowers single; (1) Flowers paired; (2) Clusters of four-seven flowers. The number of inflorescence were scored with the following: (0) Flowers few axillary; (1) Flowers terminal; (2) Loose to compact. Corolla shape were scored with the following: (0) Infundibuliform ; (1) Bilabiate ; (2) Tubular. Ancestral character state reconstruction was employed using RAxML trees (including nuclear and cpDNA data) with mapping options in Mesquite v.3.51 (Maddison and Maddison, 2011). The one-parameter Markov k-state evolution model was used for discrete unordered characters (Lewis, 2001).

Data accessibility

Raw Illumina data from target enrichment is available at the Sequence Read Archive (SRA) under accession SUB9202627 (see Table S1 for individual sample SRA accession numbers). DNA alignments, phylogenetic trees and results from all analyses and datasets can be found in the Dryad data repository.

RESULTS

Exon assembly

The number of assembled exons per species ranged from 253 (*A. macrotera* var. *parvifolia* E45) to 992 (*A. uniflora* E46) (with > 75% of the target length), with an average of 851 exons per sample (Table 1; Fig. S1). The number of exons with paralog warnings ranged from 6 in *A. macrotera* var. *parvifolia* E45 to 698 in *A. uniflora* E46 (Table 1). The concatenated alignment had a length of 365,330 bp, including 22,045 parsimony-informative sites, and a matrix occupancy of 83% (Table 2). The smallest locus had a length of 150 bp and the largest 3,998 bp. The cpDNA alignment resulted in a matrix of 163,130 bp with 3,850 parsimony-informative sites and a matrix occupancy of 96% (Table 2).

Phylogenetic reconstruction

We recovered the *Abelia* phylogeny based on nuclear and cpDNA datasets (Figs. 2, 3 and S2). Despite the generally well-supported topology, the position of clades representing *A.* × *grandiflora*, *A. uniflora* and *A. macrotera* clade were unstable across all analyses.

Phylogenetic reconstruction based on nuclear concatenation data showed all of the major clades with relationships well supported (BS ≥ 75%; Fig. 2). *Abelia schumannii* was nested within *A. macrotera*; *A. chinensis* forms a clade with *A.* × *grandiflora*; and *A. macrotera* var. *mairei* was sister to *A. uniflora*. The *A. chinensis* + *A.* × *grandiflora* clade was then sister to the *A. macrotera* var. *mairei* + *A. uniflora* clade (Fig. 2).

For the ASTRAL tree, the coalescent nuclear phylogeny recovered strong support (local posterior probabilities (LPP ≥ 0.95) for all major clades. Similar to the ML concatenation nuclear tree topology, *A. schumannii* was nested within *A. macrotera* (Fig. 3). The *A. chinensis* + *A.* × *grandiflora* clade was sister to the *A. macrotera* var. *mairei* + *A. uniflora* clade. The *A. macrotera* + *A. schumannii* clade was sister to the clade of *A.chinensis* + *A.* × *grandiflora* + *A. macrotera* var. *mairei* + *A. uniflora*. Furthermore, *Abelia forrestii* was sister to the *A. macrotera* + *A. schumannii* clade (Fig. 3). The QS analysesconfirmed the *Abelia* having strong QS support (0.7/1/1)(Fig. 3) . The clade composed of *A. chinensis* + *A.* ×

grandiflora has moderate QS support with signal for a possible alternative topology (0.33/0.06/0.99). The clade composed of *A. macrotera* var. *mairei* + *A. uniflora* has strong QS support but a signal of a possible alternative topology (0.98/0/1). The clade composed of *A. macrotera* + *A. schumannii* has strong QS support (0.94/1/0.99). The sister relationship of the clade of *A. macrotera* var. *mairei* + *A. uniflora* and the clade of *A. forrestii* have QS counter support as a clear signal for alternative topology (-0.21/0.32/0.99).

In the cpDNA tree, *A. schumannii* was sister to *A. macrotera*, the QS analysis showed moderate support (0.27/0.18/0.91). *Abelia uniflora* was sister to *A. macrotera* var. *mairei*, the clade had strong QS support as a clear signal for alternative topology (0.51/0.35/0.98). The *A. chinensis* + *A.* × *grandiflora* clade constituted the sister relationship with the *A. macrotera* var. *mairei* + *A. uniflora* +*A. macrotera* + *A. schumannii* clade, the clade has strong QS support (0.75/0.51/0.98). The results strongly support *A. forrestii* from Yunnan as sister to the remainder of this genus with the QS analysis providing full support (1/–/1) (Fig. S2).

In our species network analyses (including both 15-taxa and 12-taxa), any of the networks with one to five reticulations events were a better model than a strictly bifurcating tree (Table 2; Figs. S3 and S4). Four reticulation events were inferred for the best networks in the 15-taxa tree, with this best species network, the first reticulation event involves *A.* × *grandiflora* E159 and the *A. macrotera* clade. The second to fourth reticulation event also reveal ancestral gene flow in the *A.*× *grandiflora* clade (Fig. 4A). In the 12-taxa tree (We removed the known hybrids from the previous analyses, excluding *A.* × *grandiflora* E159, *A.*× *grandiflora* E227 and *A.*× *grandiflora* E206; Fig. 4B), the best network had three reticulations events. Here, we found there was abundant discordance in the backbone of *Abelia*; and the 12-taxa analyses showed that *A macrotera*, *A. uniflora* and *A chinensis* were each derived from independent hybrid origins.

Divergence time estimation

Divergence time estimates based on the nuclear species tree suggested that the crown group of *Abelia* originated 31.02 Ma (95% HPD: 27.57-37.10 Ma, node 1 in Fig. 5). We

found the different ages of the root had no effect on divergence time estimates (Fig. 5). The split between *A. macrotera* and *A. schumannii* was 6.78 Ma (95% HPD: 4.92-11.29 Ma, node 7 in Fig. 5). The split between *A. uniflora* and *A. macrotera* var. *mairei* was 16.12 Ma (95% HPD: 13.12-20.06 Ma, node 5 in Fig. 5). The crown of *A. forrestii* was 4.46 Ma (95% HPD:1.88-6.71 Ma, node 8 in Fig. 5). Most diversification events within *Abelia* dated back to the Early to Middle Miocene (Fig. 5). A comparison of the time estimates using the chloroplast tree is shown in Figs. 6. For instance, the age of the crown group of *Abelia* was dated to 45.10 Ma (95% HPD: 31.82-50.09 Ma, node 1 in Fig. 6). The split between *A. uniflora* and *A. macrotera* var. *mairei* was 35.07 Ma (95% HPD: 13.12-20.06 Ma, node 4 in Fig. 6). The split between *A. macrotera* and *A. schumannii* was 31.79 Ma (95% HPD: 18.39-38.15 Ma, node 5 in Fig. 6).

Ancestral area reconstruction

The results of the reconstruction of ancestral ranges are shown in Fig. 7. Our analyses revealed five dispersal events and two vicariance events among the three defined biogeographic areas (Fig. 7). The ancestor of *Abelia* was inferred to have been present throughout region A (Yunnan, Chongqing, Sichuan, Guizhou and Hubei) and B (Jiangxi and Fujian) during the Middle Miocene (Fig. 7), with subsequent dispersal or vicariance across southeast China. The results indicate a southwest China origin for the genus *Abelia* during the Eocene/Oligocene boundary.

Ecological niche modelling and niche identity tests

The AUC test (mean ± SD) for the ENM, averaged across all 25 runs, was high (0.996 ±0.000 for *A. chinensis*, 0.993 ± 0.000 for *A. forrestii*, 0.992 ± 0.000 for *A. macrotera*, 0.993± 0.001 for *A. uniflora* and 0.995 ± 0.000 for *A. schumannii*) (Figs. 8 and S5). Projections of the species niche in the LGM climate produced considerably different maps of the probability of occurrence compared to the present time. In general, with the two LGM models, large

areas appear suitable in mainland China for all species. For the CCSM and MPI model, the distribution density and range of *Abelia* under the MPI model were slightly lower than the distribution density and range under the CCSM model, but the differences were not significant (Fig. S5). The potential range for *Abelia* species in mainland China would have been much smaller, while habitats would have remained stable across most of the current distribution.

Character evolution

The number of epicalyx bracts, the number of flowers, inflorescence and corolla shape have traditionally been used for generic recognition within *Abelia*. A summary of character states that are relevant for the taxonomy of the group is shown in Figs. S6-9. Exploration of character changes and ancestral-state inference were undertaken using the tree from the nuclear and cpDNA analysis. Likelihood inferences of character states indicate that the four selected morphological characters (the number of epicalyx bracts, the number of flowers, inflorescence and corolla shape) show some level of homoplasy in *Abelia.* In nuclear analysis, our results suggest that epicalxy bracts, inflorescence and corolla shape have little homoplasy, but the ancestral character of epicalxy bracts was most likely four epicalxy, the ancestral character of inflorescence was most likely a terminal flower, and the ancestral character of corolla shape was most likely infundibuliform(Figs. S6-7). The flower type relative to corolla shows particularly high homoplasy (Fig.S7), we inferred shift from an ancestrally single flower to paired flowers in *A. chinensis* (Fig.S7).A summary of character states using the chloroplast gene tree that are relevant for the taxonomy of the group are shown in Figs. S8-9. In the cpDNA analysis, our results suggest that epicalxy bracts, inflorescence, corolla shape and flower have high homoplasy(Figs. S8-9). The ancestral state for the four character were uncertain due to the diversity in types among the major early-diverging clades. For epicalxy bracts, most likely four epicalxy was ancestral(Fig. S8). The ancestral character of inflorescence was most likely terminal flowers, the ancestral character of corolla shape was most likely infundibuliform(Figs.S8-9). The evolution of flower type was similarly complex

(Fig. 9), we inferred the ancestral character of flower typewas most likely single flower. Overall, we found that the patterns of character evolution from nuclear gene tree and cpDNA tree were similar.

DISCUSSION

Phylogenetic relationships within Abelia

This study reconstructed well-supported phylogenetic relationships for *Abelia* using both nuclear and cpDNA data (Figs. 2-3 and S2). The inferred topologies of the four recognized species in the nuclear (Astral tree and nuclear concatenation RAxML tree) and cpDNA (cpDNA RAxML tree) were different from each other (Figs. 2-3 and S2). For instance, in the nuclear concatenated RAxML tree and Astral tree, *Abelia schumannii* was nested within *A. macrotera*, and *A. macrotera* var. *mairei* is sister to the *A. uniflora* clade (Figs. 2-3). For the cpDNA RAxML tree, *A. schumannii* was sister to *A. macrotera*, and *A. macrotera* var. *mairei* is sister to the *A. uniflora* clade (Fig.2).

Because different parts of the genome have different evolutionary histories, evaluating species relationships becomes more difficult. Therefore, the different 'gene trees' obtained from different loci are often in conflict with each other and with the true species tree. When incomplete lineage sorting (ILS) is present, gene trees can differ from each other and from the species tree, presenting substantial challenges to phylogeny estimation methods (Degnan and Rosenberg, 2009; Edwards, 2009). Empirical and simulation studies have shown this to have an effect on phylogeny estimation (Chou et al., 2015; Tonini et al., 2015) especially with the choice of methods (concatenation or species tree) (Xi et al., 2014). For phylogenetic analyses to accurately reconstruct organismal history (i.e., the species tree), orthologous sequences need to be compared (Wendel and Doyle, 1998).

According to the phylogenetic tree reconstructed from our nuclear and cpDNA data, we found that *A. uniflora* is sister to *A. macrotera* var. *mairei*, and *A. schumannii* is nested in *A. macrotera* (Figs. 2A-B, Fig. 3). In addition, their nodes have strong QS support values. Our

results are consistent with Jacobs et al. (2010) in terms of *A. schumannii* being nested within *A. macrotera.* Landrein(2020) reported that the *A. uniflora* group contains *A. macrotera* var. *mairei*. Additionally, *A. schumannii* has no independent ecological niche, and its distribution overlaps with *A. macrotera* (Landrein et al., 2020). We also found that *A. schumannii* and *A. macrotera*, *A. uniflora* and *A. macrotera* var. *mairei* have many similarities in morphology (i.e. single-flowered inflorescence, red corolla, and two sepals). We thus propose the merging of *A. schumannii* with and *A. macrotera* and also the merging of *A. macrotera* var. *mairei* with *A. uniflora*, resulting in recognizing four species with *Abelia*: *A. chinensis*, *A. uniflora*, *A. macrotera* and *A. forrestii.* Of course, we have only sampled one *A. schumannii* accession and our sampling is not enough to definitively place *A. schumannii* as a synonym. For more accurate and robust results we need more samples, which is a direction of our future research.

Hybridization within Abelia

Abelia chinensis has an infundibuliform corolla with exserted stamens and style. An initial aim of breeders was to make *A. chinensis* cold tolerant by crossing it with taxa thought to have originated from colder areas in China. This first breeding gave rise to *A.* × *grandiflora*, a widely cultivated taxon of *Abelia* in temperate regions. The origin of *A.* × *grandiflora* has been documented by André (1886) 'Seen in the M.M. Rovelli Brothers Nurseries in Pallanza (Lake Maggiore)'. The morphology of this taxon strongly suggests a of hybrid origin between *A. chinensis* and *A. uniflora*. More recent crosses used *A. schumannii* with *A. chinensis*, which led to the creation of several possible backcrosses (Landrein et al., 2017). *Abelia uniflora* is the most enigmatic species in the genus though it was only briefly described by(Wallich, 1829) and was the first taxon to be introduced into cultivation.

Abelia uniflora is often difficult to identify from morphological characters alone and shows a disjunct distribution in the border between Jiangxi and Fujian (Landrein et al., 2017). West-East China disjunctions have also been recorded in different genera and species, and some were hypothesized as allopatric incipient speciation (Qiu et al., 2009). The

morphological differences among entities within the *A. uniflora* complex may be explained by one or several historical or ongoing evolutionary processes. One possible explanation is that the *A. uniflora* complex represents a single, hyperdiverse species. As a hyperdiverse species, *A. uniflora* would likely exhibit genetic panmixia or high levels of gene flow due to more-or-less continuous contact among populations (Hamrick and Godt, 1990; Constance and William, 1991). The *A. uniflora* complex as a single hyperdiverse species comprises a null taxonomic hypothesis (Link-Pérez, 2010) while the alternative is that speciation has occurred or is occurring. If speciation exists, we expect to detect clear genetic differentiation, which may be stronger if speciation is complete, or weaker if it is ongoing or confounded by introgression (Nosil, 2008; Liu et al., 2018).

Isolation of *A. forrestii* within the deep valleys of the Nu-Jiang (Salween) and the Yangtze Rivers allowed for limited introgression followed by allopatric speciation. This species possesses a more specialized long tubular corolla that may have coevolved with specific pollinators (Landrein and Prenner, 2016). *Abelia chinensis* and *A. forrestii* are morphologically similar, both having five sepals and more tubular flowers; characters that have infiltrated from hybridization and introgression with *A. macrotera*, *A. schumannii* and *A. chinensis* (Landrein et al., 2017). Likelihood inference indicates evolutionary patterns of morphological characters. Based on morphological evidence and AFLP data, Landrein *et al*. (2017) indicated that *A. uniflora* shows evidence of formation due to hybridization and introgression between *A. macrotera* and *A. chinensis*. Examples of similar speciation events in different families were cited in Li et al. (2011), and the hypothesis put forward was glaciation survival east and west of the Mekong-Salween divide. Glaciation may have led to the isolated distribution of *A. forrestii.* Repeated hybridization and introgression tend to blur the lines between hybrids and their parents and Landrein et al (2017) showed that *A. forrestii* occurs in a clear zone of hybridization is present at the contact zone between *A. macrotera* and *A. chinensis* leading to the hypothesis that hybridization and introgression between *A. macrotera* and *A. chinensis* led to the emergence of *A. forrestii.*

Diversification history of *Abelia*

Molecular clock estimation suggests that the crown of *Abelia* dates to the Early Oligocene 31.02 Ma (95% HPD: 27.57-37.10 Ma) (Fig. 5). In addition, previous phylogenetic and phylogeographic studies generally showed that the existing populations of many species in Taiwan were descendants of mainland China (e.g., Taiwania, Chou, et al., 2011; *Sassafras*, Nie, et al., 2007; *Dichocarpum arisanense*, Xiang et al., 2017; *Triplostegia*, Niu et al., 2018), with no cases supporting a reverse dispersal direction having been reported. Ancestral area reconstruction revealed that the *A. uniflora* complex might have colonized Southwest China, Central-East China, and Taiwan during the Oligocene (Fig. 7). For the *A. uniflora* complex, multiple asynchronous expansions, multiple independent refugia *in situ* and complex topography in this region might be responsible for the undetectable mismatch in the distribution analyses (Cun and Wang, 2010; Yan et al., 2012; Shao et al., 2015). The time of these diversification events (about 55.51 Ma and 46.26 Ma, respectively) predate the uplift of the Hengduan Mountains (Xing and Ree, 2017). The uplift of QTP was a consequence of the collision of the Indian subcontinent with the Eurasian plate 40-50 million years ago (Yin and Harrison, 2000; Fu et al., 2020) and subsequent Quaternary climatic oscillations altered the distribution patterns of organisms as well as affected biodiversity (Qiu et al., 2011). It is hypothesized that uplift of the QTP, which started during the Middle Eocene and continued into the mid-Pliocene, created conditions for the origin and divergence of multitudinous species in the QTP and adjacent regions (Qiu et al., 2011).

Our ENM analysis provides a detailed picture of the last glacial cycle (Fig. 7). The results indicate that species differentiation in *Abelia* occurred in the Oligocene, suggesting that extant populations likely differentiated well before the LGM. Therefore, the climatic shock in the LGM may have had a significant impact on the recent history of *Abelia* at a population level compared with the previous period of species differentiation (Qiu et al., 2011; Qi et al., 2012). Potential suitable habitat for *A. forrestii* was distributed mainly over Southwest China during the LGM period. However, it is now only distributed in Yunnan and Sichuan of Southwest China with altitudes ranging from 1900 to 3300 m. Additionally, based

on ENM analysis, *A. chinensis* expanded to the coastal regions of East China and reached Taiwan via land bridges in the Taiwan Strait during the glacial period. Due to repeated glacial-interglacial cycles, mainland China and Taiwan populations may have experienced frequent gene flow through a continental bridge during the Quaternary. Because *Abelia* does not have a strong ability of pollen or seed transmission, the present distributional pattern of *A. forrestii* may be the result of topographic isolation and postglacial contraction.

Our phylogenetic analyses indicate that *A. chinensis* var. *ionadra* from Taiwan is sister to *A. chinensis* from Jiangxi China (Fig. 7). The distribution patterns of the two taxa thus represent a disjunction between southern Taiwan and mainland China (Fig. 6). Based on our time estimates, the Taiwanese *A. chinensis* var. *ionadra* dates to the Middle Miocence, ca. 19.33 Ma (Fig. 5), which greatly predates the formation of Taiwan, beginning in the Late Miocene (Sibuet and Hsu, 2004). A similar disjunction predating the formation of Taiwan is shown by *Tinospora dentata* which split from its Japanese relatives in the Early Oligocene, 38.97 Ma (95% HPD: 26.45-52.52) (Wang et al., 2017).

Taiwan is located at the eastern edge of the Eurasian plate and the Taiwan Strait could have first occurred in the Late Mesozoic (Ye, 1982; Suo et al., 2015). Owing to the intense tectonic movements, contacts between Taiwan and mainland China occurred during the Late Cretaceous-Early Paleocene and Late Eocene-Early Oligocene (Teng, 1992; Zhang, 1995). It has been suggested that tropical rainforests in the Indo-Malayan region may have appeared near the K-Pg boundary (Wang et al., 2012). Macrofossils of some plants, closely related to extant subtropical species, have been reported from the Early Miocene of Taiwan, whereas pollen fossils can date to the Oligocene (Li, 2000), although their geographic sources remain disputed (Huang, 2011). Due to the landmass being subjected to stretching and rifting (Ye, 1982; Teng, 1992; Suo et al., 2015) and an increasingly cooler climate in Asia during the Late Eocene(Zachos et al., 2001), a vicariance event may have occurred between Taiwan and mainland China around that time. Part of the mountain ranges in Taiwan are a relict area for the ‘Taiwan-Sinzi Folded Zone’ (Ye, 1982; Teng, 1992). Thus, our data from *Abelia* suggests that the flora of the Taiwan (Yilan) might contain relatively ancient components. It has been

acknowledged that the flora of mainland China has contributed to the floristic assembly of Taiwan (Li and Keng, 1950; Hsieh, 2002). However, only in the Late Miocene (9-6 Ma) did the Luzon arc began to collide with the Eurasian plate (Sibuet et al., 2002). Thus, we hypothesize that the relatively young components of the flora of Taiwan (Yilan) might have originated from mainland China, whereas more ancient components were from mainland China alone. This hypothesis remains to be further tested by studying additional plant groups, especially ancient lineages, through integration of phylogenetic and molecular dating methods.

CONCLUSIONS

Robust phylogenetic relationships were consistently reconstructed within *Abelia* based on comprehensive taxon sampling, using both nuclear and chloroplast data. The nuclear and cpDNA phylogenies show *A. schumannii* nested within the *A. macrotera*, and *A. macrotera* var. *mairei* is sistre with *A. uniflora*. Also, there was plenty of discordance in the backbone of *Abelia*, and the network(12-taxa) analyses shows that *A. macrotera*, *A. uniflora*, and *A chinensis* are all from independent hybrid origins. This is a potential reason why the taxonomy of this group is so complicated. Cyto-nuclear discordance was uncovered at shallow phylogenetic levels. According to nuclear and chloroplast data, as well as morphological similarity, we suggest that *A. schumannii* be regarded as a synonym of *A. macrotera*, and *A. macrotera* var. *mairei* be regarded as a synonym of *A. uniflora*.

We used molecular dating, biogeographical and ENM methods to explored how geology and climate together influenced the evolutionary history of *Abelia*, which is an ecologically sensitive and cold-adapted herbaceous genus. High genetic divergences were detected among *Abelia* populations in Southwest China, Central China, and Taiwan, and several interglacial refugia were recognized in the central Hengduan Mountains. Ancestral area reconstruction revealed that *Abelia* originated in Southwest China, and diversification began during the Middle Eocene, then colonized Central China in the mid-Oligocene, and finally dispersed to

Taiwan by a land bridge at approximately 19.33 Ma. Based on phylogeographic and ENM analyses, frequent gene flow might have existed between mainland China and Taiwan populations with repeated continued distribution between the two regions. In summary, our findings, together with those from other studies in this region (Han et al., 2016), suggest that, apart from geographic barriers, local adaptation to different climatic conditions appears to be one of the major drivers for lineage diversification of plants endemic to East Asian land-bridge islands. Our research represents the first comprehensive phylogeographic study on herbaceous plants to investigate the Taiwan and mainland China disjunction and supports that postglacial range contraction together with topographic heterogeneity resulted in the Taiwan and China mainland disjunction.

TAXONOMIC TREATMENT

Landrein et al. (2017, 2020) recognize *Abelia* as including *A. chinensis*, *A. forrestii*, *A. schumannii*, *A. macrotera* and *A. uniflora*. Our nuclear phylogenies strongly show that *A. schumannii* was nested within *A. macrotera*, and *A. macrotera* var. *mairei* was nested within *A. uniflora*. Additionally, the distribution area and morphological characters of *A. schumannii* overlap with or are similar to *A. macrotera*, and the distribution area and morphological characters of *A. macrotera* var. *mairei* overlap or are similar to *A. uniflora*. Based on phylogenetic relationships, morphological characters, ancestral area reconstructions and divergence time, we propose to merge *A. schumannii* into *A. macrotera*, and *A. macrotera* var. *mairei* into *A. uniflora*.

Abelia macrotera (Graebn. et Buchw.) Rehder, Pl. Wilson. (Sargent) 1(1): 126 (1911). - Type:

Abelia schumannii (Graebn.) Rehder, Pl. Wilson. (Sargent) 1(1): 121 (1911).

=*Linnaea schumannii* Graebn., Bot. Jahrb. Syst. 29: 130. 1900. Lectotype here designated: China, Sichuan, Garze Tibetan Aut. Pref., Kangding Xian, Lucheng, Pratt, A.E. 271 (Lectotype K!, Isolectotypes A!, BM!, E!, P!)

=*Linnaea tereticalyx* Graebn. et Buchw. ex Graebn., Bot. Jahrb. Syst. 29: 130. 1900; *Abelia tereticalyx* (Graebn.) Rehder, in Sargent, Pl. Wilson. 1: 127. 1911. Lectotype here designated: China. Sichuan: Garze Tibetan Aut. Pref., Kangding Xian, Lucheng, Pratt, A.E. 136 (Lectotype K, Isolectotypes BM!, E!, P!)

Description: shrubs. Leaves ovate, rarely elliptic. Leaf margin entire or with a few irregular gland-tipped teeth and the blade often grey-green abaxially with sparsely hairy. Flowers axillary. Peduncles densely pilose. Calyx lobes 2. Sepals often reddish with 3-5 main veins and with a ciliate margin. Corolla bilabiate and infundibuliform, red-purple Base of corolla tube bulging ventrally. Corolla lobes subequal. Stamens 4. Filaments adnate to lower part of corolla tube, hairy basally. Ovary longitudinally ribbed, ventrally compressed and widened along the fertile locule. Style glabrous to sparsely hairy at base, inserted to slightly exserted from the corolla tube, stigmas capitate, white and papillose. Fruit an achene with persistent, slightly accrescent and spreading sepals. Achenes, flattened ventrally and ridged.

Distribution. -Qingcheng Shan, Leshan and Ya'an Prefectures.

Abelia uniflora R. Br. in Wall., Pl. As. Rar. 1. 15. 1830. -Type: holotype: CGE.

= *Abelia mairei* H. Lév., Cat. Pl. Yun-Nan: 26 (Léveillé 1916).

=*Abelia macrotera* (Graebn. & Buchw.) Rehder var. *mairei* (H. Lév.) *Landrein* **comb. et stat. Nov.**

Type: China, Yunnan, ['Siao Ou Long'], E. E. Maire 6 (holotype E!).

Description: Shrub, young shoots hirsute. Leaves with a serrate margin. Corolla with a long narrow tube widening gradually to themouth, markings reaching the corolla tube; sepals acute.

Distribution. -China.

Author contributions

H.F.W. and J.W. conceived the study. H.F.W. and D.F.M-B. performed the research and analyzed the data. Q.H.S., D.F.M-B., H.X.W., J.W. J.B.L, and H.F.W. wrote and revised the

manuscript.

Acknowledgement

The work was funded by National Scientific Foundation of China (31660055). We appreciate Gabriel Johnson for his help with the target enrichment experiment, and the United States National Herbarium for permission for sampling some collections. We acknowledge the staff in the Laboratories of Analytical Biology at the National Museum of Natural History, the Smithsonian Institution for support and assistance.

REFERENCE

Bell CD, Donoghue MJ. 2005. Phylogeny and biogeography of Valerianaceae (Dipsacales) with special reference to the South American valerians. *Org Divers Evol* 5:147-159

Birky CWJr. 1995. Uniparental inheritance of mitochondrial and chloroplast genes: mechanisms and evolution. *Proceedings of the National Academy of Sciences, USA* 92: 11331-11338.

Cao YN, Wang IJ, Chen LY, Ding YQ, Liu LX, Qiu YX. 2018. Inferring spatial patterns and drivers of population divergence of Neolitsea sericea (Lauraceae), based on molecular phylogeography and landscape genomics. *Molecular phylogenetics and evolution*, 126, 162-172.

Chou YW, Thomas PI, Ge XJ, LePage BA, Wang CN. 2011. Refugia and phylogeography of Taiwania in East Asia. *Journal of Biogeography* 38:1992-2005

Chou J, Gupta A, Yaduvanshi S, Davidson R, Nute M, Mirarab S, Warnow T. 2015. A comparative study of SVDquartets and other coalescent-based species tree estimation methods. *BMC genomics*, 16(10), 1-11.

Constance IM, William JL. 1991. "Strategies for conserving clinal, ecotypic, and disjunct population diversity in widespread species" in Genetics and Conservation of Rare Plants, ed. D. A. Falk. Oxford: Oxford University Press, 283.

Cun YZ, Wang XQ. 2010. Plant recolonization in the Himalaya from the southeastern

Qinghai-Tibetan Plateau: geographical isolation contributed to high population differentiation. *Molecular Phylogenetics and Evolution* 56: 972-982.

Chen ZD, Ying JS, Lu AM. 2012. Disjunct distribution of seed plants between southwestern China and Taiwan island of China. *Chinese Bulletin of Botany*, 47: 551-570.

Chen XD, Yang J, Feng L, Zhou T, Zhang H, Li HM, Bai GQ, Meng X, Li ZH, Zhao GF. 2020. Phylogeography and population dynamics of an endemic oak (Quercus fabri Hance) in subtropical China revealed by molecular data and ecological niche modeling. *Tree Genetics* & *Genomes* 16:2.

Corriveau JL, Coleman AW. 1988. Rapid screening method to detect potential biparental inheritance of plastid DNA and results for over 200 angiosperms. *American Journal of Botany* 75: 1443-1458.

Doyle JJ, Doyle J. 1987. A rapid DNA isolation procedure for small quantities of fresh leaf tissue. *Phytochemical Bulletin* v.19, p.11-15.

Degnan JH, Rosenberg NA. 2009. Gene tree discordance, phylogenetic inference and the multispecies coalescent. *Trends in Ecology & Evolution*, 26, 332-340.

Drummond AJ, Suchard MA, Xie D, Rambaut A. 2012. Bayesian phylogenetics with BEAUti and the BEAST 1.7. *Molecular Biology Evolution* 29: 1969-1973.

Fu PC, Sun SS, Khan G, Dong XX, Tan JZ, Favre A, Chen SL. 2020. Population subdivision and hybridization in a species complex of Gentiana in the Qinghai-Tibetan Plateau. *Annals of botany* 125(4), 677-690.

Givnish TJ, Renner SS. 2004. Tropical intercontinental disjunctions: Gondwana breakup, immigration from the boreotropics, and transoceanic dispersal.

Edwards SV. 2009. Is a new and general theory of molecular systematics emerging? *Evolution*, 63, 1-19.

Hamrick JL, Godt MW. 1990. “Allozyme diversity in plant species,” in Plant Population Genetics, Breeding, and Genetic Resources, eds A. H. D. Brown, M. T. Clegg, A. L. Kahler, and B. S. Weir. Sunderland, MA: Sinauer, 43-63.

Hsieh CF. 2002. Composition, endemism and phytogeographical affinities of the

Taiwan flora. *Taiwania* 47: 298-310.

Huang S. 2011. Historical biogeography of the flora of Taiwan. *Journal of the National Taiwan Museum* 64(3): 33-63.

Jacobs B, Pyck N, Smets E. 2010. Phylogeny of the Linnaea clade: are Abelia and Zabelia closely related? *Molecular Phylogenetics and Evolution* 57: 741-752.

Jiang XL, Hipp AL, Deng M, Su T, Zhou ZK, Yan MX. 2019. East Asian origins of European holly oaks (*Quercus* section *Ilex* Loudon) via the Tibet□Himalaya. *Journal of Biogeography* 46(10): 2203-2214.

Kim TJ, Sun BY, Park CW, Suh Y. 1998. Phylogenetic implications of matK sequences in Caprifoliaceae. *American Journal of Botany* 86 (Suppl.) 3202 (Abstract 86).

Kalyaanamoorthy S, Minh BQ, Wong TK, Von Haeseler A, Jermiin LS. 2017. ModelFinder: fast model selection for accurate phylogenetic estimates. *Nature methods* 14(6), 587-589.

Katoh K, Standley DM. 2013. MAFFT multiple sequence alignment software version 7: improvements in performance and usability. *Molecular biology and evolution* 30(4): 772-780.

Landrein S, Prenner G, Chase MW, Clarkson JJ. 2012. *Abelia* and relatives: phylogenetics of Linnaeeae (Dipsacales-Caprifoliaceaemsl) and a new interpretation of their inflorescence morphology. *Botanical Journal of the Linnean Society* 169(4): 692-713.

Landrein S, Buerki S, Wang HF, Clarkson JJ. 2017. Untangling the reticulate history of species complexes and horticultural breeds in *Abelia* (Caprifoliaceae). *Annals of Botany* 2: 257-269.

Landrein S, Prenner G. 2016. Structure, ultrastructure and evolution of floral nectaries in the Taiwaninflower tribe Linnaeeae and related taxa (Caprifoliaceae). *Botanical Journal of the Linnean Society* 181: 37-69.

Landrein S, Farjon A. 2020**.** A monograph of Caprifoliaceae: Linnaeeae. *Kew Bulletin*, 74(4): 1-197.

Lanfear R, Frandsen PB, Wright AM, Senfeld T, Calcott B. 2017. PartitionFinder 2: new

methods for selecting partitioned models of evolution for molecular and morphological phylogenetic analyses. *Molecular Biology and Evolution* 34: 772-773.

Li J, Milne RI, Ru D, Miao J, Tao W, Zhang L, Mao K. 2020. Allopatric divergence and hybridization within Cupressus chengiana (Cupressaceae), a threatened conifer in the northern Hengduan Mountains of western China. *Molecular Ecology*. doi: https://doi.org/10.1111/mec.15407.

Li HL, Keng H. 1950. Phytogeographical affinities of southern Taiwan. *Taiwania* 1: 103-128.

Li CY. 2000. *A study on Miocene floras in Taiwan* (Doctoral dissertation, Ph. D. Thesis, National Chung Hsing University, Taichung, Taiwan, 1-115 (in Chinese).

Lichter-Marck IH, Freyman WA, Siniscalchi CM, Mandel JR, Castro-Castro A, Johnson G, Baldwin BG. 2020. Phylogenomics of Perityleae (Compositae) provides new insights into morphological and chromosomal evolution of the rock daisies. *Journal of Systematics and Evolution*.

Liu JQ, Sun YS, Ge XJ, Gao LM, Qiu YX. 2012. Phylogeographic studies of plants in China: advances in the past and directions in the future. *Journal of Systematic and Evolutionary* 50: 267-275.

Liu YP, Ren ZM, Harris AJ, Peterson PM, Wen J, Su X. 2018. Phylogeography of Orinus (Poaceae), a dominant grass genus on the Qingha-Tibet Plateau. *Botanical Journal of the Linnean Society* 186(2): 202-223.

Linder PH, Antonelli A, Humphreys AM, Pirie MD, Wüest RO. 2013. What determines biogeographical ranges? Historical wanderings and ecological constraints in the danthonioid grasses. *Journal of Biogeography* 40(5): 821-834.

Lu SY, Peng CI, Cheng YP, Hong KH, Chiang TY. 2001. Chloroplast DNA phylogeography of *Cunninghamia konishii* (Cupressaceae), an endemic conifer of Taiwan. *Genome* 44(5): 797-807.

Lee-Yaw JA, Grassa CJ, Joly S, Andrew R L, Rieseberg LH. 2019. An evaluation of alternative explanations for widespread cytonuclear discordance in annual sunflowers (Helianthus). *New Phytologist* 221(1), 515-526.

Miller MA, Pfeiffer W, Schwartz T. 2010. Creating the CIPRES Science Gateway for inference of large phylogenetic trees. Gateway Computing Environments Workshop, pp.1-8.

Manchester SR. 1995. Update on the megafossil flora of Florissant, Colorado. In *Fossil flora and stratigraphy of the Florissant Formation, Colorado. Proceedings of the Denver Museum of Nature and Science*, series 4:137-162.

Manchester SR. 2000. Late Eocene fossil plants of the John Day Formation, Wheeler County, Oregon. *Oregon Geology* 62: 51-63.

Mandel JR, Dikow RB, Funk VA, Masalia RR, Staton SE, Kozik A,Burke JM. 2014. A target enrichment method for gathering phylogenetic information from hundreds of loci: an example from the Compositae. *Applications in plant sciences* 2(2): 1300085.

Mummenhoff K, Linder P, Friesen N, Bowman JL, Lee JY, Franzke A. 2004. Molecular evidence for bicontinental hybridogenous genomic constitution in *Lepidium* sensu stricto (Brassicaceae) species from Australia and New Zealand. *American Journal of Botany* 91(2): 254-261.

Morales-Briones DF, Liston A, and Tank DC. 2018. Phylogenomic analyses reveal a deep history of hybridization and polyploidy in the Neotropical genus Lachemilla (Rosaceae). New Phytologist, 218(4), 1668-1684.

Morales-Briones DF, Gehrke B, Huang CH, Liston A, Ma H, Marx HE, ... and Yang Y. 2020. Analysis of paralogs in target enrichment data pinpoints multiple ancient polyploidy events in Alchemilla sl (Rosaceae). bioRxiv.

Nathan R, Schurr FM, Spiegel O, Steinitz O, Trakhtenbrot A, Tsoar A. 2008. Mechanisms of long-distance seed dispersal. *Trends in ecology & evolution* 23(11): 638-647.

Niu YT, Ye JF, Zhang JL, Wan JZ, Yang T, Wei XX, Lu LM, Li JH, Chen ZD. 2018. Long-distance dispersal or postglacial contraction? Insights into disjunction between Himalaya-Hengduan Mountains and Taiwan in a cold-adapted herbaceous genus, *Triplostegia*. *Ecology and Evolution* 8: 1131-1146.

Nie ZL, Sun H, Li H, Wen J. 2007. Intercontinental biogeography of subfamily Orontioideae (Symplocarpus, Lysichiton, and Orontium) of Araceae in eastern Asia and North America. *Molecular Phylogenetics and Evolution* 40: 155-165.

Nosil P. 2008. Speciation with gene flow could be common. *Molecular ecology,* 17(9): 2103-2106.

Nguyen LT, Schmidt HA, von Haeseler A, Minh, BQ. 2015. IQ-TREE: a fast effective stochastic algorithm for estimating maximum-likelihood phylogenies. *Molecular Biology and Evolution* 32, 268-274. doi: https://doi.org/10.1093/molbev/msu300

Neves LG, Davis JM, Barbazuk WB, Kirst M. 2013. Whole-exome targeted sequencing of the uncharacterized pine genome. *The Plant Journal* 75: 146-156.

Phillips SJ, Anderson RP, Schapire RE. 2006. Maximum entropy modeling of species geographic distributions. *Ecological modelling* 190(3-4): 231-259.

Pouchon C, Fernández A, Nassar JM, Boyer F, Aubert S, Lavergne S, Mavárez J. 2018. Phylogenomic analysis of the explosive adaptive radiation of the Espeletia complex (*Asteraceae*) in the tropical Andes. *Systematic Biology* 67: 1041-1460.

Qiu YX, Guan BC, Comes HP. 2009. Did glacials and/or interglacials promote allopatric incipient speciation in East Asia temperate plants? Phylogeographic and coalescent analyses on refugial isolation and divergence in Dysosma versipellis. *Molecular Phylogenetics and Evolution* 51: 281-293.

Qiu YX, Fu CX, Comes HP, 2011. Plant molecular phylogeography in China and adjacent regions: Tracing the genetic imprints of Quaternary climate and environmental change in the world's most diverse temperate flora. *Molecular Phylogenetics and Evolution* 59: 225-244.

Qian H, Ricklefs RE. 2004. Geographical distribution and ecological conservatism of disjunct genera of vascular plants in eastern Asia and eastern North America. *Journal of Ecology*, 92(2): 253-265.

Raven PH, Axelrod DI. 1974. Angiosperm biogeography and past continental movements. *Annals of the Missouri Botanical Garden* 61(3): 539-673.

Santorum JM, Darriba D, Taboada GL and Posada D. 2014. jmodeltest. org: selection of nucleotide substitution models on the cloud. Bioinformatics 30(9): 1310-1311.

Swets JA. 1988. Measuring the accuracy of diagnostic systems. *Science* 240:1285-1293.

Smith SA, Dunn CW. 2008. Phyutility: a phyloinformatics tool for trees, alignments and molecular data. *Bioinformatics* 24: 715-716.

Shao YZ, Chen Y, Zhang XC, Xiang QP. 2015. Species delimitation and phylogeography of the *Abies chensiensis* complex inferred from morphological and molecular data. *Botanical Journal of the Linnean Society* 177: 175-188.

Sibuet JC, Hsu SK, Le Pichon X, Le Formal JP, Reed D, Morre G, Liu CS. 2002. East Asia plate tectonics since 15 Ma: constraints from the Taiwan region. *Tectonophysics* 344: 103-134.

Sibuet JC, Hsu SK. 2004. How was Taiwan created? *Tectonophysics* 379: 159-181.

Stamatakis A. 2014. RAxML version 8: a tool for phylogenetic analysis and post analysis of large phylogenies. *Bioinformatics* 30: 1312-1313.

Stephens JD, Rogers WL, Mason CM, Donovan LA, Malmberg RL. 2015. Species tree estimation of diploid *Helianthus* (Asteraceae) using target enrichment. *American Journal of Botany* 102(6): 910-920.

Suo YH, Li SZ, Zhao SJ, Somerville ID, Yu S, Dai LM, Xu LQ, Cao XZ, Wang PC. 2015. Continental margin basins in East Asia: tectonic implications of the Meso-Cenozoic East China Sea pull-apart basins. *Geological Journal* 50: 139-156.

Sugiura N. 1978. Further Analysis of the Data by Akaike's Information Criterion and the Finite Corrections. *Communications in Statistics-Theory and Methods* 7: 13-26.

Shi Y, Cui Z, Su Z. 2006. The Quaternary glaciations and environmental variations in China. Hebei Science and Technology Press, Shijiazhuang 65-101.

Šarhanová P, Sharbel TF, Sochor M, Vašut RJ, Dančák M and Trávníček B. 2017. Hybridization drives evolution of apomicts in Rubus subgenus Rubus: evidence from microsatellite markers. *Annals of botany* 120(2), 317-328.

Teng LS. 1992. Geotectonic evolution of Tertiary continental margin basins of Taiwan.

Petroleum Geology of Taiwan 27: 1-19.

Thomas DC, Chatrou LW, Stull GW, Johnson DM, Harris DJ, Thongpairoj US., Saunders RM. 2014. The historical origins of palaeotropical intercontinental disjunctions in the pantropical flowering plant family Annonaceae. *Perspectives in plant ecology, evolution and systematics* 17(1): 1-16.

Tonini J, Moore A. Stern D, Shcheglovitova M, Ortí G. 2015. Concatenation and species tree methods exhibit statistically indistin-guishable accuracy under a range of simulated conditions. *PLoS Currents Edition* 1.

Wang HF, Landrein S, Dong WP, Nie ZL, Kondo K, Funamoto T, Wen J, Zhou SL. 2015. Molecular phylogeny and biogeographic diversification of Linnaeoideae (Carprifoliaceae *s.l.*) disjunctively distributed in Eurasia, North American and Mexico. *PLoS One* 10: e0116485.

Wang HX, Liu H, Moore MJ, Landrein S, Liu B, Zhu ZX, Wang HF. 2020a. Plastid phylogenomic insights into the evolution of the *Caprifoliaceae s.l.* (Dipsacales). *Molecular Phylogenetics and Evolution* 142: 106641.

Wang HX, Morales-Brionesb DF, Moore MJ. Wen J, Wang HF. 2020b. A phylogenomic perspective on gene tree conflict and character evolution in Caprifoliaceae using target enrichment data, with Zabelioideae recognized as a new subfamily. doi: https://doi.org/10.1101/2020.10.29.359950

Wang HX, Morales-Brionesb DF, Moorec MJ, Wen J, Wang HF. 2021. A phylogenomic perspective on gene tree conflict and character evolution in Caprifoliaceae using target enrichment data, with Zabelioideae recognized as a new subfamily. doi: https://doi.org/10.1111/jse.12745.

Wang J, Feng C, Jiao T, Von Wettberg EB, Kang M. 2017. Genomic Signature of Adaptive Divergence despite Strong Nonadaptive Forces on Edaphic Islands: A Case Study of Primulina juliae. *Genome Biology and Evolution* 9(12): 3495-3508.

Wang IJ. 2013. Examining the full effects of landscape heterogeneity on spatial genetic variation: a multiple matrix regression approach for quantifying geographic and

ecological isolation. *Evolution* 67:3403-3411.

Wang W, Ortiz RDC, Jacques FM, Xiang XG, Li H., Lin L, Chen ZD. 2012. Menispermaceae and the diversification of tropical rainforests near the Cretaceous-Paleogene boundary. *New Phytologist* 195(2): 470-478.

Wei XX, Yang ZY, Li Y, Wang XQ. 2010. Molecular phylogeny and biogeography of *Pseudotsuga* (Pinaceae): insights into the floristic relationship between Taiwan and its adjacent areas. *Molecular Phylogenetics and Evolution* 55(3): 776-785.

Wen J, Wagner WL. 2020. Collections-based systematics and biogeography in the 21st century. *Journal of Systematics and Evolution* 58 (6): 743-750.

Wen J, Nie ZL,Ickert□Bond SM. 2019. Advances in biogeography in the age of a new modern synthesis. *Journal of Systematics and Evolution* 57 (6): 543-546.

Wen J. 2001. Evolution of eastern Asian-eastern North American biogeographic disjunctions: a few additional issues. *International Journal of Plant Sciences* 162(S6), S117-S122.

Wen J, Ree RH, Ickert-Bond SM, Nie Z, Funk V. 2013. Biogeography: where do we go from here? *Taxon* 62(5): 912-927.

Weitemier K, Straub SCK, Cronn RC, Fishbein M, Schmickl R, McDonnell A, Liston A. 2014. Hyb-Seq: combining target enrichment and genome skimming for plant phylogenomics. *Applications in Plant Sciences* 2: 9, dio: https://doi.org/10.3732/apps.1400042.

Wu CY. 1987. Origin and evolution of flora of Xizang. Flora Xizangica. *Science Press, Beijing*, 879-902.

Wu PC, Wang MZ. 2001. Relationship of the tropical elements of the bryophytes between Hengduan Mts., southwest China and Taiwan province, southeast China. *Guizhou Science* 19(4): 6-9.

Xu J, Deng M, Jiang XL, Westwood M, Song YG, Turkington R. 2015. Phylogeography of Quercus glauca (Fagaceae), a dominant tree of East Asian subtropical evergreen forests, based on three chloroplast DNA interspace sequences. *Tree Genet Genomes*

11(1): 805.

Xi ZL, Liu JS. 2014. Coalescent versus concatenation methods and the placement of Amborella as sister to water lilies. *Systematic Biology* 63: 919-932 .

Xiang KL, Zhao L, Erst AS, Yu SX, Jabbour F, Wang W. 2017. A molecular phylogeny of *Dichocarpum* (Ranunculaceae): Implications for eastern Asian biogeography. *Molecular Phylogenetics and Evolution* 107: 594-604.

Xiang CL, Dong HJ, Landrein S, Zhao F, Yu WB, Soltis DE, Peng H.1998. Revisiting the phylogeny of Dipsacales: new insights from phylogenomic analyses of complete plastomic sequences. *Journal of Systematics and Evolution* doi: https:// doi.org/10.1111/jse.12526.

Xiang QY, Soltis DE. 2001. Dispersal-vicariance analyses of intercontinental disjuncts: historical biogeographical implications for angiosperms in the Northern Hemisphere. *International Journal of Plant Sciences* 162(S6): S29-S39.

Xing Y, Ree RH. 2017. Uplift-driven diversification in the Hengduan Mountains, a temperate biodiversity hotspot. *Proceedings of the National Academy of Sciences* 114(17): E3444-E3451.

Xue JY, Wang Y, Chen M, Dong S, Shao ZQ, Liu Y. 2020. Maternal Inheritance of U's Triangle and Evolutionary Process of Brassica Mitochondrial Genomes. *Frontiers in plant science* 11, 805.

Yan HF, Zhang CY, Wang FY, Hu, CM, Ge XJ, Hao G. 2012. Population expanding with the phalanx model and lineages split by environmental heterogeneity: a case study of *Primula obconica* in subtropical China. *PLoS One* 7: e41315.

Yang JB, Li DZ, Li HT. 2014. Highly effective sequencing whole chloroplast genomes of angiosperms by nine novel universal primer pairs. *Molecular Ecology Resources* 14(5), 1024-1031.

Yang Q, Landrein S. 2011. *Linnaeaceae. In,Wu,Z.,Hong,D.,Raven,P.H. (Eds.), Flora of China*,vol. 19. Science Press and Missouri Botanical Garden Press, Beijing and St.Louis 642-648.

Ye XQ. 1982. On the formation and development of the geology and geomorphology of Taiwan. J. Central China Teachers College 83-89.

Ye WQ, Yap ZY, Li P, Comes HP, Qiu YX. 2018. Plastome organization, genome-based phylogeny and evolution of plastid genes in Podophylloideae (Berberidaceae). *Molecular phylogenetics and evolution* 127: 978-987.

Ye Z, Zhu G, Chen P, Zhang D, Bu W. 2014. Molecular data and ecological niche modelling reveal the P leistocene history of a semi-aquatic bug (*M icrovelia douglasi douglasi*) in E ast A sia. *Molecular ecology* 23(12): 3080-3096.

Ye XY, Ma PF, Yang GQ, Guo C, Zhang YX, Chen YM, Li DZ. 2019. Rapid diversification of alpine bamboos associated with the uplift of the Hengduan Mountains. *Journal of Biogeography* 00: 1-12.

Ye J, Lu L, Liu B, Yang T, Zhang J, Hu H, Chen Z. 2019. Phylogenetic delineation of regional biota: A case study of the Chinese flora. *Molecular phylogenetics and evolution* 135: 222-229.

Yu Y, Harris AJ, Blair C, He X. 2015. RASP (Reconstruct Ancestral State in Phylogenies): a tool for historical biogeography. *Molecular Phylogenetics and Evolution* 87: 46-49.

Yin A, Harrison TM. 2000. Geologic evolution of the Himalayan Tibetan orogen. *Annual Review of Earth and Planetary Sciences* 28: 211-280.

Yoder AD, Nowak MD. 2006. Has vicariance or dispersal been the predominant biogeographic force in Madagascar? Only time will tell. *Ecology Evolution and Systematics* 37: 405-431.

Zhang C, Rabiee M, Sayyari E, Mirarab S. 2018. ASTRAL-III: polynomial time species tree reconstruction from partially resolved gene trees. BMC Bioinformatics. 19: 523.

Zhang HD. 1995. *Floristic analysis of Taiwan*. In: Editorial Corpus of Zhang Hongda (Ed.), Corpus of Zhang Hongda. Sun Yatsen University Press, Guangzhou, pp: 131-146.

Zachos J, Pagani M, Sloan L, Thomas E, Billups K. 2001. Trends, rhythms, and aberrations in global climate 65 Ma to present. *Science* 292: 686-693.

Figure Legends

Figure 1. Photographs of *Abelia* taxa. (A, D, G) *A.* × *grandiflora*; note 5 sepals with large white flowers; (B, E) *Abelia* 'Rose Creek', note the dense terminal inflorescence and campanulate corolla; (C) *Abelia chinensis* note five sepals with small white flowers, bees gather nectar from flowers; (F) Birds feed on nectar; (H, I) *Abelia* 'Edward rose', note the two sepals and the notched apex.

Figure 2. Tanglegram of the nuclear concatenated (left) and plastid (right phylogenies. Dotted lines connect taxa between the two phylogenies. Maximum likelihood bootstrap support values are shown above branches. The asterisks indicate maximum likelihood bootstrap support of 100%. Major taxonomic groups or main clades in the family as currently recognized are indicated by branch colors as a visual reference to relationships.

Figure 3. ASTRAL-III species tree; Clade support is depicted as: QC/QD/QI/LPP.

Figure 4. Best supported species networks inferred with Phylonet for the (A) 15-taxa, (B) 12-taxa. Numbers next to the inferred hybrid branches indicate inheritance probabilities.

Figure 5. BEAST analysis of divergence times based on the species tree of the nuclear data. Calibration points are indicated by A, B. Numbers 1-8 represent major divergence events in *Abelia*; mean divergence times and 95% highest posterior densities are provided for each.

Figure 6. BEAST analysis of divergence times based on cpDNA matrix. Calibration points are indicated by A, B. Numbers 1-8 represent major divergence events in *Abelia*; mean divergence times and 95% highest posterior densities are provided for each.

Figure 7. Ancestral area reconstruction for *Abelia*. Areas of endemism are as follows: (A) Southwest China, (B) Central-East China, (C) Taiwan and Ryukyu Islands. The numbered nodes represent crown nodes of important colonization events, as discussed in the text.

Figure 8. Comparison of potential distributions as probability of occurrence for *A. chinensis*, *A. forrestii*, *A. macrotera*, *A. uniflora* and *A. schumannii* at the CCSM climatic scenarios of the Last Glacial Maximum (LGM, ca. 21,000 years BP). The maximum training

sensitivity plus specificity logistic threshold has been used to discriminate between suitable (cutline 0.1-1 areas) and unsuitable habitat. The darker color indicates a higher probability of occurrence.

Fig. S1 Heatmaps showing gene recovery efficiency for the nuclear gene in 45 species of *Abelia*. Columns represent genes, and each row is one sample. Shading indicates the percentage of the reference locus length coverage.

Fig. S2 cpDNA RAxML tree; Clade support is depicted as: QC/QD/QI/LPP.

Fig. S3 Best species networks of the selective nuclear dataset estimated with PhyloNet for the 15-taxa. A: One hybridization event; B: Two hybridization events; C: Three hybridization events; D: Four hybridization events; F: Five hybridization events. Blue branches connect the hybrid nodes. Numbers next to blue branches indicate inheritance probabilities.

Fig. S4 Best species networks of the selective nuclear dataset estimated with PhyloNet for the 12-taxa. A: One hybridization event; B: Two hybridization events; C: Three hybridization events; D: Four hybridization events; F: Five hybridization events. Blue branches connect the hybrid nodes. Numbers next to blue branches indicate inheritance probabilities.

Fig. S5 Potential distribution probability (in logistic value) of occurrence for *Abelia* in East Asia.

Fig. S6 Likelihood inference of character evolution in *Abelia* using Mesquite v.2.75 based on nuclear matrix. Left, Inflorescence; Right, Corolla shape.

Fig. S7 Likelihood inference of character evolution in *Abelia* using Mesquite v.2.75 based on nuclear matrix. Left, The number of epicalxy bracts; Right, The number of flowers.

Fig. S8 Likelihood inference of character evolution in *Abelia* using Mesquite v.2.75 based on cpDNA matrix. Left, Inflorescence; Right, Corolla shape.

Fig. S9 Likelihood inference of character evolution in *Abelia* using Mesquite v.2.75 based on cpDNA matrix. Left, The number of epicalxy bracts; Right, The number of flowers.

Table. 1 Dataset statistics, including the number of taxa, number of characters, number of PI characters, missing data.

Table. 2 HybPiper assembly statistics

Table. 3 Model selection of the different species networks and bifurcating trees.

Table. S1 List of species and vouchers used in this study.

Table. S2 19 bioclimatic variables for ENM analyses

Table. S3 HybPiper assembly statistics

Table 1. Dataset statistics, including the number of taxa, number of characters, number of PI characters, missing data.

Alignment	No. of taxa	No. sites	Missing data (%)	No. of variable/Parsimony informative sites
Nuclear	45	365,330	16.88	43,248/22,045
cpDNA	45	163,130	4.35	7,926/3,850

Table 2. HybPiper assembly statistics

Species	Number of reads	Number of reads on target	Percent reads on target	Number of exons with reads	Number of exons with contigs	Number of exons with sequences	Number of exons with sequences > 25% of the target length	Number of exons with sequences > 50% of the target length	Number of exons with sequences > 75% of the target length	Number of exons with sequences > 150% of the target length	Number of exons with paralog warnings
A. chinensis E111	12086904	4547698	0.376	1094	1010	985	983	966	907	0	123
A. chinensis E119	14252558	4342227	0.305	1098	999	972	970	957	906	1	93
A. chinensis var. *ionandra* E30	8512137	2058453	0.242	1054	969	945	942	917	835	1	72
A. chinensis var. *ionandra* E33	15488895	4871294	0.315	1094	999	973	971	960	915	2	86
A. chinensis var. *ionandra* E166	3560876	749920	0.211	1057	966	948	941	893	763	1	60
A. chinensis var. *ionandra* E167	4799543	1123534	0.234	1103	982	962	960	930	863	1	96
A. chinensis var. *ionandra* E229	8420983	2523313	0.3	1110	1014	985	983	963	914	1	90
A. chinensis var. *ionandra* E230	11800314	4525033	0.383	1121	1012	983	982	967	927	2	93
A. chinensis var. *ionandra* E231	9802195	1723306	0.176	1155	1036	1012	1011	994	941	3	140
A. forrestii E36	32830208	9311224	0.284	1160	1051	1011	1010	994	954	1	159
A. forrestii E37	9666409	2890168	0.299	1114	1005	977	975	961	921	0	78
A. × *grandiflora* E159	9807596	3364549	0.343	1121	1027	997	995	975	930	1	219
A. × *grandiflora* E206	9076240	3538761	0.39	1118	1021	994	993	979	930	1	162
A. × *grandiflora* E227	12254174	4742077	0.387	1133	1039	1010	1010	993	944	1	271
A. macrotera E110	9134947	2888390	0.316	1072	988	960	959	940	901	1	94
A. macrotera var. *deutziaefolia* E153	7647999	2528861	0.331	1125	1016	985	982	954	893	0	95
A. macrotera var. *deutziaefolia* E154	10129358	3237016	0.32	1130	1016	979	978	963	921	0	100
A. macrotera var. *deutziaefolia* E155	4426579	1033080	0.233	1103	987	966	962	933	860	0	70
A. macrotera var. *deutziaefolia* E156	9536952	3305495	0.347	1130	1017	978	977	959	918	0	102
A. macrotera var. *deutziaefolia* E157	4754995	1345791	0.283	1096	988	959	958	943	892	1	89
A. macrotera var. *deutziaefolia* E158	9445133	2856721	0.302	1113	1009	971	969	953	915	0	100

A. macrotera var. *engleriana* E34	7200184	1795642	0.249	1099	1003	971	970	953	905	1	83
A. macrotera var. *engleriana* E149	11394102	3988828	0.35	1114	1020	986	984	968	920	0	99
A. macrotera var. *engleriana* E347	8183348	1385872	0.169	1103	990	960	958	941	893	0	82
A. macrotera var. *engleriana* E349	6925508	1478921	0.214	1105	993	966	966	943	863	0	73
A. macrotera var. *mairei* E3	5493922	1344879	0.245	1076	987	963	963	946	904	1	88
A. macrotera var. *mairei* E43	6885612	1741233	0.253	1085	1000	971	971	956	914	1	87
A. macrotera var. *mairei* E211	4278814	878749	0.205	1068	978	949	946	921	846	0	68
A. macrotera var. *parvifolia* E6	5223871	1429204	0.274	1063	990	959	958	938	874	0	83
A. macrotera var. *parvifolia* E45	1833543	32422	0.018	825	436	424	417	355	253	0	6
A. uniflora E46	16490536	3625219	0.22	1133	1064	1042	1042	1028	992	0	698
A. uniflora E47	3257944	439031	0.135	1068	945	924	924	904	858	1	120
A. uniflora E48	1922338	260996	0.136	958	734	715	696	587	423	0	19
A. uniflora E51	18769946	3613529	0.193	1086	991	967	966	946	892	2	103
A. uniflora E52	2713371	576730	0.213	1039	954	930	929	913	871	1	80
A. uniflora E53	2724962	439041	0.161	1038	943	921	920	902	855	0	75
A. uniflora E54	15998204	2846753	0.178	1079	992	968	967	943	900	1	103
A. schumannii E44	2391304	253742	0.106	1038	897	877	874	847	775	0	67
Diabelia sanguinea E303	10970170	3075238	0.28	1134	1025	991	988	973	914	0	91
*D. serrat*a E321	13220295	4190116	0.317	1138	1037	1002	1000	986	934	0	93
Dipelta floribunda E55	4636783	105360	0.023	924	660	642	639	601	507	0	27
D. floribunda E56	6580640	248258	0.038	992	853	833	830	793	680	0	43
Kolkwitzia amabilis E9	9779050	2641147	0.27	1097	1005	984	983	967	916	0	75
Linnaea borealis E14	9523146	1355451	0.142	1069	981	962	961	946	902	1	73
Vesalea occidentalis E96	6434742	142056	0.022	974	730	712	703	650	559	0	23

Table 3. Model selection of the different species networks and bifurcating trees.

Topology	lnL	Parameters	Loci	Number of hybridizations	Information criteria		
					AIC	AICc	BIC
15 taxa							
nuclear ASTRAL	-4177.949631	27	167	N/A	8409.899262	8420.776960	8494.085095
nuclear RAxML	-4148.054160	27	167	N/A	8350.108319	8360.986017	8434.294152
cpDNA	-4231.190608	27	167	N/A	8516.381215	8527.258913	8600.567048
Network 1	-4088.228145	29	167	1	8234.456290	8247.157020	8324.878111
Network 2	-4050.799135	31	167	2	8163.598270	8178.294566	8260.256078
Network 3	-3948.351402	33	167	3	7962.702804	7979.574984	8065.596600
Network 4	**-3932.455932**	**35**	**167**	**4**	**7934.911864**	**7954.148505**	**8044.041647**
Network 5	-3935.844300	37	167	5	7945.688601	7967.487050	8061.054372
12 taxa							
nuclear ASTRAL	-2716.350474	21	162	N/A	5474.700949	5481.300949	5539.540472
nuclear RAxML	-2724.448876	21	162	N/A	5490.897753	5497.497753	5555.737276
cpDNA	-2723.043552	21	162	N/A	5488.087104	5494.687104	5552.926627
Network1	-2660.433072	23	162	1	5366.866143	5374.866143	5437.880859
Network2	-2601.023466	25	162	2	5252.046932	5261.605756	5329.236841
Network3	**-2549.319250**	**27**	**162**	**3**	**5152.638500**	**5163.922082**	**5236.003601**
Network4	-2552.995453	27	162	3	5159.990906	5171.274488	5243.356007
Network 5	-2606.591029	27	162	3	5267.182058	5278.465640	5350.547159

Table. S1 List of species and vouchers used in this study.

Order	Ingroup/ Outgroup	Taxon	Coding	Locality	Voucher specimen number	SRA accession
1	Ingroup	*Abelia chinensis*	B	Jiujiang, Jiangxi, China	HUTB, E119	SRR13890741
2	Ingroup	*Abelia chinensis*	B	Jiujiang, Jiangxi, China	HUTB, E111	SRR13890742
3	Ingroup	*Abelia chinensis* var. *ionandra*	C	Keelung Islet,Taiwan, China	HUTB, E30	SRR13705776
4	Ingroup	*Abelia chinensis* var. *ionandra*	C	Amami Islands, Japan	HUTB, E33	SRR13890725
5	Ingroup	*Abelia chinensis* var. *ionandra*	C	Okinawa Island, Okinawa, Japan	HUTB, E166	SRR13890726
6	Ingroup	*Abelia chinensis* var. *ionandra*	C	Yilan, Taiwan, China	HUTB, E167	SRR13890744
7	Ingroup	*Abelia chinensis* var. *ionandra*	C	Yilan,Taiwan, China	HUTB, E229	SRR13890743
8	Ingroup	*Abelia chinensis* var. *ionandra*	C	Yilan, Taiwan, China	HUTB, E230	SRR13890751
9	Ingroup	*Abelia chinensis* var. *ionandra*	C	Yilan, Taiwan, China	HUTB, E231	SRR13890745
10	Ingroup	*Abelia forrestii*	A	Nujiang, Yunnan, China	HUTB, E36	SRR13890748
11	Ingroup	*Abelia forrestii*	A	Nujiang, Yunnan, China	HUTB, E37	SRR13705787
12	Ingroup	*Abelia grandiflora*	A	Zhengzhou, Henan, China	HUTB, E159	SRR13890724
13	Ingroup	*Abelia grandiflora*	B	Beijing Botanical Garden, Beijing	HUTB, E206	SRR13705765
14	Ingroup	*Abelia grandiflora*	B	Zhengzhou, Henan, China	HUTB, E227	SRR13890730
15	Ingroup	*Abelia macrotera*	A	Emei, Sichuan, China	HUTB, E110	SRR13705799
16	Ingroup	*Abelia macrotera* var. *deutziaefolia*	A	Fuyang, Guizhou, China	HUTB, E153	SRR13890758
17	Ingroup	*Abelia macrotera* var. *deutziaefolia*	A	Fuyang, Guizhou, China	HUTB, E154	SRR13890757
18	Ingroup	*Abelia macrotera* var. *deutziaefolia*	A	Fuyang,Guizhou, China	HUTB, E155	SRR13890727
19	Ingroup	*Abelia macrotera* var. *deutziaefolia*	A	Fuyang, Guizhou, China	HUTB, E156	SRR13890731
20	Ingroup	*Abelia macrotera* var. *deutziaefolia*	A	Fuyang, Guizhou, China	HUTB, E157	SRR13890728
21	Ingroup	*Abelia macrotera* var. *deutziaefolia*	A	Fuyang, Guizhou, China	HUTB, E158	SRR13890729
22	Ingroup	*Abelia macrotera* var. *engleriana*	A	Nanchuan, Chongqing, China	HUTB, E34	SRR13890756
23	Ingroup	*Abelia macrotera* var. *engleriana*	A	Nanchuan, Chongqing, China	HUTB, E149	SRR13890753

24	Ingroup	*Abelia macrotera* var. *engleriana*	A	Nanchuan, Chongqing, China	HUTB, E347	SRR13890755
25	Ingroup	*Abelia macrotera* var. *engleriana*	A	Nanchuan, Chongqing, China	HUTB, E349	SRR13890754
26	Ingroup	*Abelia macrotera* var. *mairei*	A	Emei, Sichuan, China	HUTB, E3	SRR13890733
27	Ingroup	*Abelia macrotera* var. *mairei*	A	Emei, Sichuan, China	HUTB, E43	SRR13890740
28	Ingroup	*Abelia macrotera* var. *mairei*	A	Emei, Sichuan, China	HUTB, E211	SRR13890732
29	Ingroup	*Abelia macrotera* var. *parvifolia*	A	Yichang, Hubei, China	HUTB, E6	SRR13890752
30	Ingroup	*Abelia macrotera* var. *parvifolia*	A	Yichang, Hubei, China	HUTB, E45	SRR13890750
31	Ingroup	*Abelia uniflora*	B	Wuyishan, Fujian, China	HUTB, E46	SRR13890738
32	Ingroup	*Abelia uniflora*	B	Wuyishan, Fujian, China	HUTB, E47	SRR13890739
33	Ingroup	*Abelia uniflora*	B	Wuyishan, Fujian, China	HUTB, E48	SRR13890734
34	Ingroup	*Abelia uniflora*	B	Wuyishan, Fujian, China	HUTB, E51	SRR13705798
35	Ingroup	*Abelia uniflora*	B	Wuyishan, Fujian, China	HUTB, E52	SRR13890736
36	Ingroup	*Abelia uniflora*	B	Wuyishan, Fujian, China	HUTB, E53	SRR13890735
37	Ingroup	*Abelia uniflora*	B	Wuyishan, Fujian, China	HUTB, E54	SRR13890737
38	Ingroup	*Abelia schumannii*	A	Ganzi, Sichuan, China	HUTB, E44	SRR13890749
39	Outgroup	*Diabelia serrata*		Takakuma, Kagoshima, Japan	HUTB, E321	SRR13890747
40	Outgroup	*Diabelia sanguinea*		Numadzu, Shizuoka, Japan	HUTB, E303	SRR13890746
41	Outgroup	*Dipelta floribunda*		Cambridge, UK.	HUTB, E55	SRR13705794
42	Outgroup	*Dipelta floribunda*		Cambridge, UK.	HUTB, E56	SRR13705795
43	Outgroup	*Kolkwitzia amabilis*		Weinan, Shanxi, China	HUTB, E9	SRR13705797
44	Outgroup	*Linnaea borealis*		Yili, Xinjiang, China	HUTB, E14	SRR13705786
45	Outgroup	*Vesalea occidentalis*		Durango, Mexico	HUTB, E96	SRR13705793

Table. S2 19 bioclimatic variables for ENM analyses

Code	Variable
BIO1	Annual Mean Temperature
BIO2	Mean Diurnal Range [Mean of monthly (max temp-min temp)]
BIO3	Isothermality (BIO2/BIO7) (* 100)
BIO4	Temperature Seasonality (standard deviation *100)
BIO5	Max Temperature of Warmest Month
BIO6	Min Temperature of Coldest Month
BIO7	Temperature Annual Range (BIO5-BIO6)
BIO8	Mean Temperature of Wettest Quarter
BIO9	Mean Temperature of Driest Quarter
BIO10	Mean Temperature of Warmest Quarter
BIO11	Mean Temperature of Coldest Quarter
BIO12	Annual Precipitation
BIO13	Precipitation of Wettest Month
BIO14	Precipitation of Driest Month
BIO15	Precipitation Seasonality (Coefficient of Variation)
BIO16	Precipitation of Wettest Quarter
BIO17	Precipitation of Driest Quarter
BIO18	Precipitation of Warmest Quarter
BIO19	Precipitation of Coldest Quarter

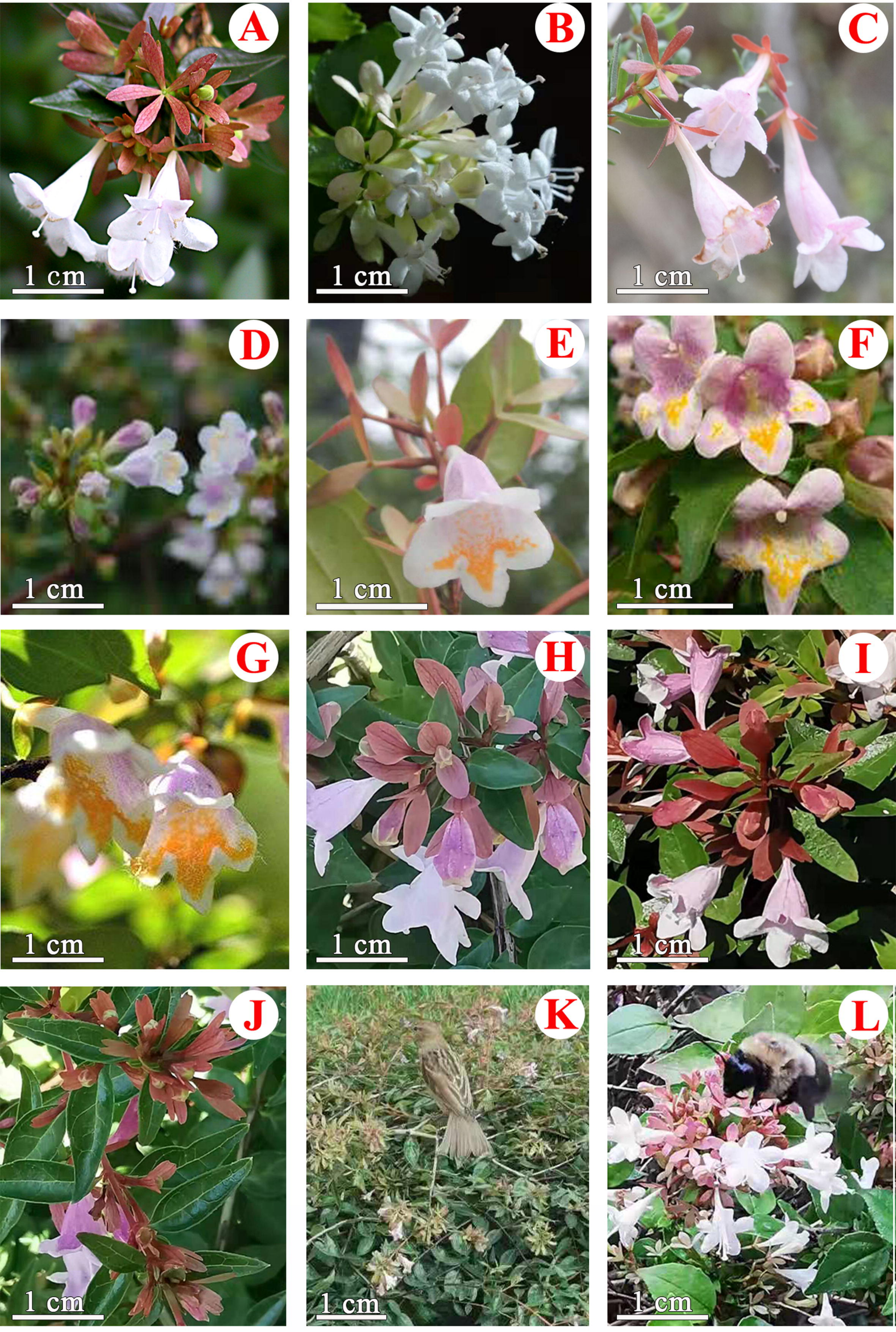
A
1 cm
B
1 cm
C
1 cm
D
1 cm
E
1 cm
F
1 cm
G
1 cm
H
1 cm
I
1 cm
J
1 cm
K
1 cm
L
1 cm

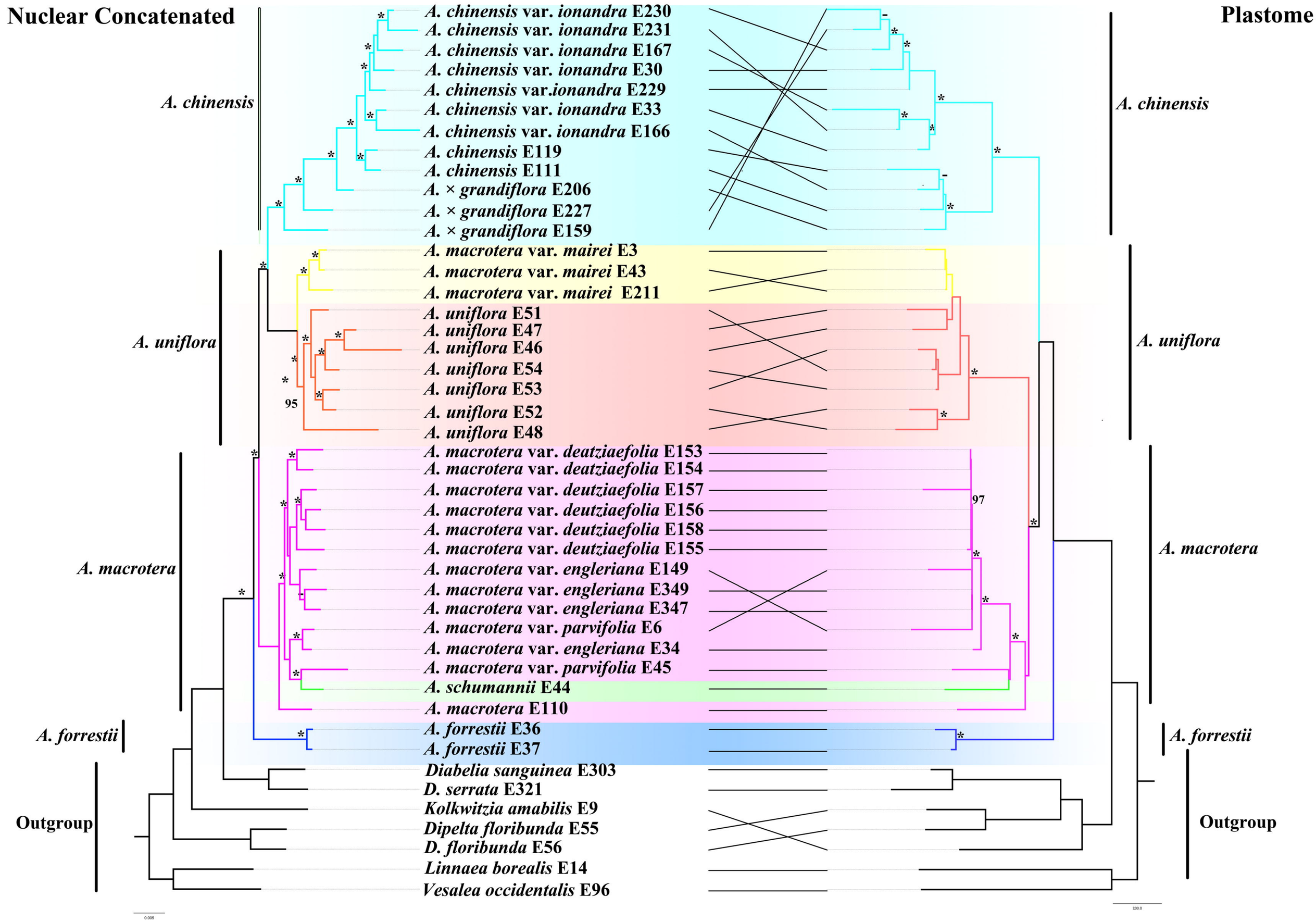
Nuclear Concatenated
Plastome
A. chinensis
A. uniflora
A. macrotera
A. forrestii
Outgroup
A. chinensis var. ionandra E230
A. chinensis var. ionandra E231
A. chinensis var. ionandra E167
A. chinensis var. ionandra E30
A. chinensis var.ionandra E229
A. chinensis var. ionandra E33
A. chinensis var. ionandra E166
A. chinensis E119
A. chinensis E111
A. × grandiflora E206
A. × grandiflora E227
A. × grandiflora E159
A. macrotera var. mairei E3
A. macrotera var. mairei E43
A. macrotera var. mairei E211
A. uniflora E51
A. uniflora E47
A. uniflora E46
A. uniflora E54
A. uniflora E53
A. uniflora E52
A. uniflora E48
A. macrotera var. deatziaefolia E153
A. macrotera var. deatziaefolia E154
A. macrotera var. deutziaefolia E157
A. macrotera var. deutziaefolia E156
A. macrotera var. deutziaefolia E158
A. macrotera var. deutziaefolia E155
A. macrotera var. engleriana E149
A. macrotera var. engleriana E349
A. macrotera var. engleriana E347
A. macrotera var. parvifolia E6
A. macrotera var. engleriana E34
A. macrotera var. parvifolia E45
A. schumannii E44
A. macrotera E110
A. forrestii E36
A. forrestii E37
Diabelia sanguinea E303
D. serrata E321
Kolkwitzia amabilis E9
Dipelta floribunda E55
D. floribunda E56
Linnaea borealis E14
Vesalea occidentalis E96
95
97
0.005
500.0

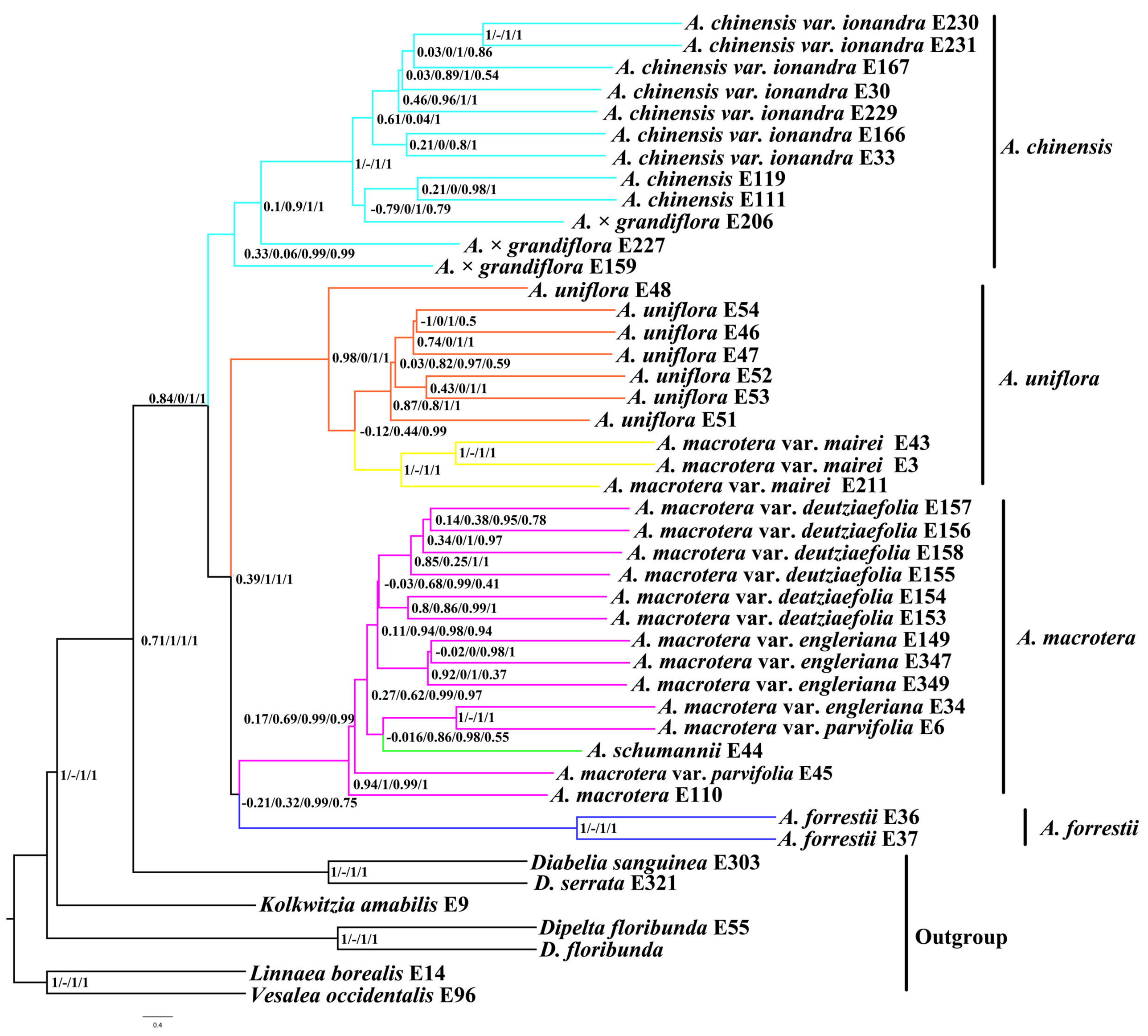
A. chinensis var. ionandra E230
A. chinensis var. ionandra E231
A. chinensis var. ionandra E167
A. chinensis var. ionandra E30
A. chinensis var. ionandra E229
A. chinensis var. ionandra E166
A. chinensis var. ionandra E33
A. chinensis E119
A. chinensis E111
A. × grandiflora E206
A. × grandiflora E227
A. × grandiflora E159
A. chinensis
A. uniflora E48
A. uniflora E54
A. uniflora E46
A. uniflora E47
A. uniflora E52
A. uniflora E53
A. uniflora E51
A. macrotera var. mairei E43
A. macrotera var. mairei E3
A. macrotera var. mairei E211
A. uniflora
A. macrotera var. deutziaefolia E157
A. macrotera var. deutziaefolia E156
A. macrotera var. deutziaefolia E158
A. macrotera var. deutziaefolia E155
A. macrotera var. deatziaefolia E154
A. macrotera var. deatziaefolia E153
A. macrotera var. engleriana E149
A. macrotera var. engleriana E347
A. macrotera var. engleriana E349
A. macrotera var. engleriana E34
A. macrotera var. parvifolia E6
A. schumannii E44
A. macrotera var. parvifolia E45
A. macrotera E110
A. macrotera
A. forrestii E36
A. forrestii E37
A. forrestii
Diabelia sanguinea E303
D. serrata E321
Kolkwitzia amabilis E9
Dipelta floribunda E55
D. floribunda
Linnaea borealis E14
Vesalea occidentalis E96
Outgroup
0.84/0/1/1
0.71/1/1/1
0.39/1/1/1
0.17/0.69/0.99/0.99
0.94/1/0.99/1
-0.21/0.32/0.99/0.75
1/-/1/1
0.1/0.9/1/1
0.33/0.06/0.99/0.99
1/-/1/1
0.61/0.04/1/1
0.21/0/0.8/1
0.21/0/0.98/1
-0.79/0/1/0.79
1/-/1/1
0.03/0/1/0.86
0.03/0.89/1/0.54
0.46/0.96/1/1
0.98/0/1/1
-1/0/1/0.5
0.74/0/1/1
0.03/0.82/0.97/0.59
0.43/0/1/1
0.87/0.8/1/1
-0.12/0.44/0.99
1/-/1/1
1/-/1/1
0.14/0.38/0.95/0.78
0.34/0/1/0.97
0.85/0.25/1/1
-0.03/0.68/0.99/0.41
0.8/0.86/0.99/1
0.11/0.94/0.98/0.94
-0.02/0/0.98/1
0.92/0/1/0.37
0.27/0.62/0.99/0.97
1/-/1/1
-0.016/0.86/0.98/0.55
1/-/1/1
1/-/1/1
1/-/1/1
1/-/1/1
0.4

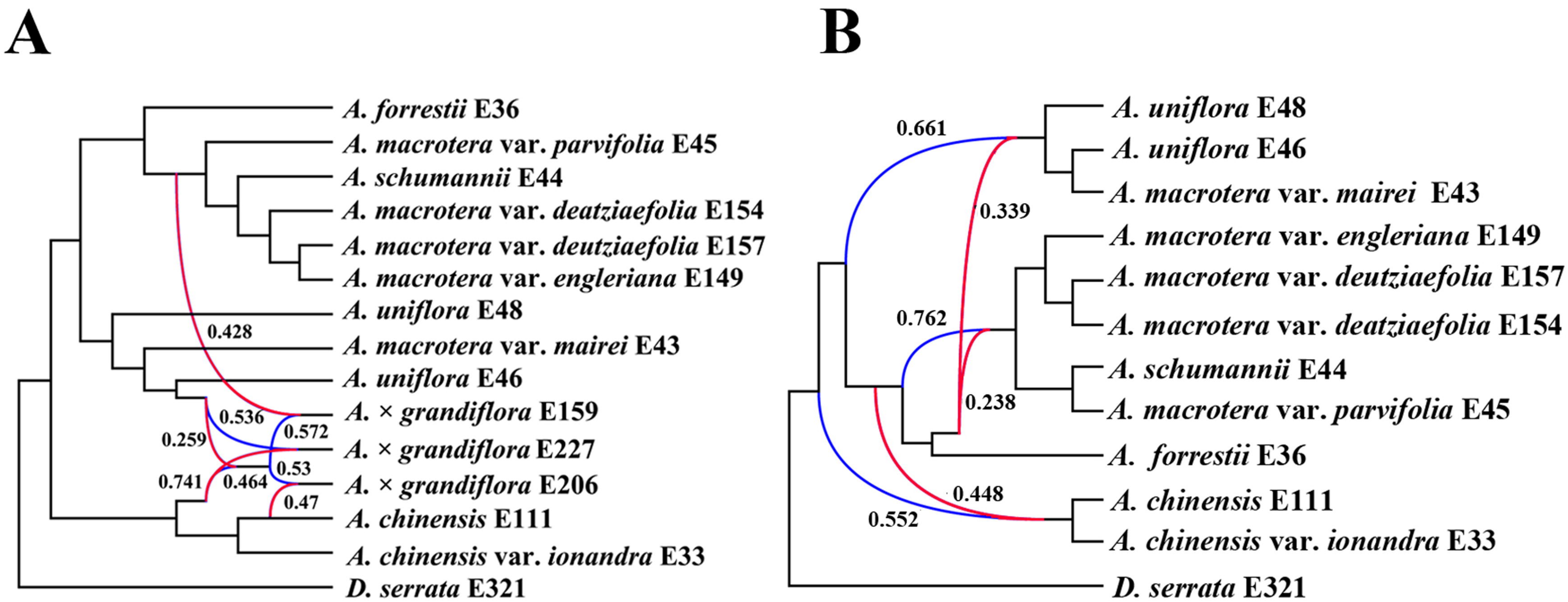
A
A. forrestii E36
A. macrotera var. parvifolia E45
A. schumannii E44
A. macrotera var. deatziaefolia E154
A. macrotera var. deutziaefolia E157
A. macrotera var. engleriana E149
A. uniflora E48
A. macrotera var. mairei E43
A. uniflora E46
A. × grandiflora E159
A. × grandiflora E227
A. × grandiflora E206
A. chinensis E111
A. chinensis var. ionandra E33
D. serrata E321
0.428
0.536
0.572
0.259
0.53
0.741
0.464
0.47
B
A. uniflora E48
A. uniflora E46
A. macrotera var. mairei E43
A. macrotera var. engleriana E149
A. macrotera var. deutziaefolia E157
A. macrotera var. deatziaefolia E154
A. schumannii E44
A. macrotera var. parvifolia E45
A. forrestii E36
A. chinensis E111
A. chinensis var. ionandra E33
D. serrata E321
0.661
0.339
0.762
0.238
0.448
0.552

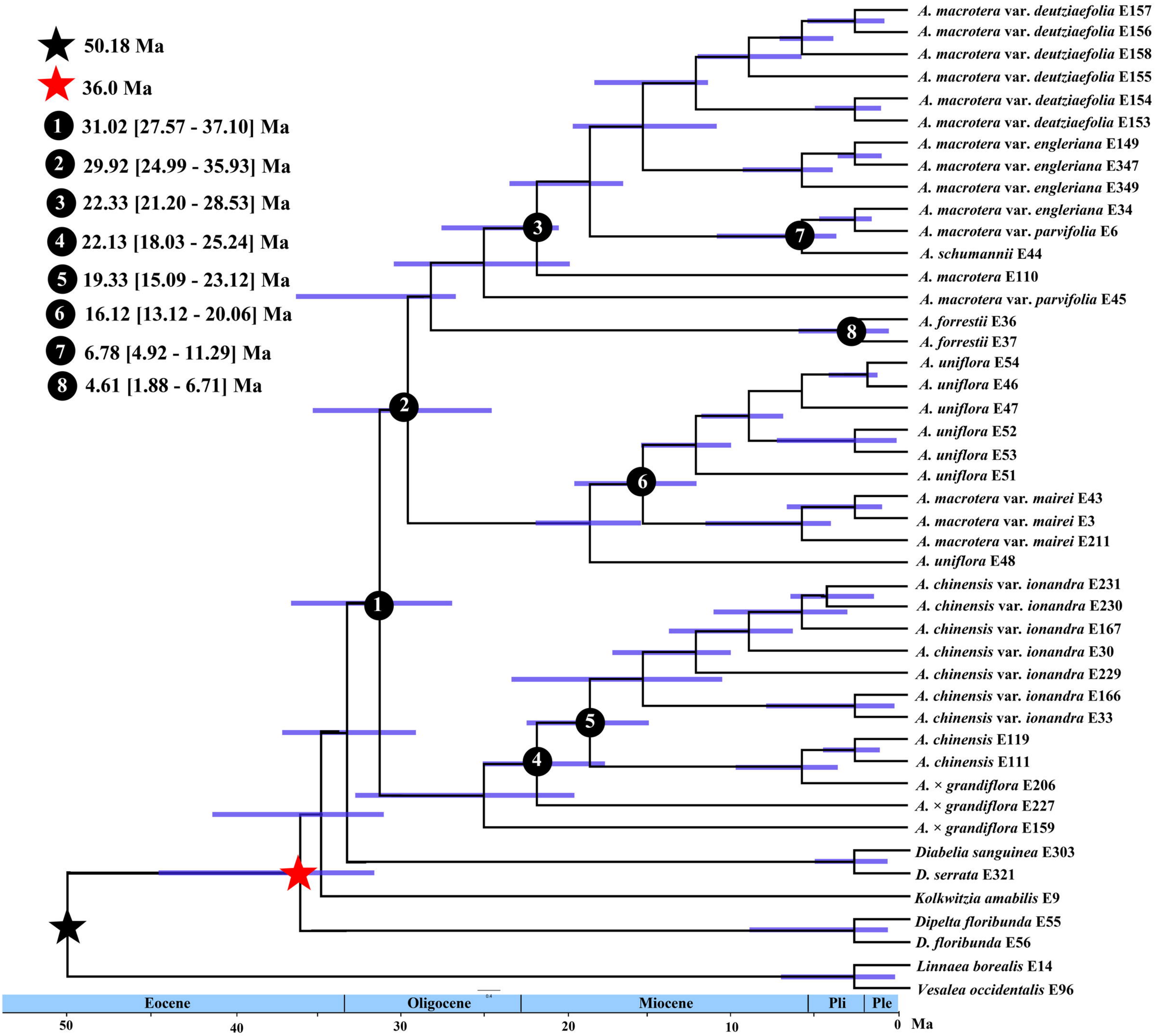
50.18 Ma
36.0 Ma
1 31.02 [27.57 - 37.10] Ma
2 29.92 [24.99 - 35.93] Ma
3 22.33 [21.20 - 28.53] Ma
4 22.13 [18.03 - 25.24] Ma
5 19.33 [15.09 - 23.12] Ma
6 16.12 [13.12 - 20.06] Ma
7 6.78 [4.92 - 11.29] Ma
8 4.61 [1.88 - 6.71] Ma
A. macrotera var. deutziaefolia E157
A. macrotera var. deutziaefolia E156
A. macrotera var. deutziaefolia E158
A. macrotera var. deutziaefolia E155
A. macrotera var. deatziaefolia E154
A. macrotera var. deatziaefolia E153
A. macrotera var. engleriana E149
A. macrotera var. engleriana E347
A. macrotera var. engleriana E349
A. macrotera var. engleriana E34
A. macrotera var. parvifolia E6
A. schumannii E44
A. macrotera E110
A. macrotera var. parvifolia E45
A. forrestii E36
A. forrestii E37
A. uniflora E54
A. uniflora E46
A. uniflora E47
A. uniflora E52
A. uniflora E53
A. uniflora E51
A. macrotera var. mairei E43
A. macrotera var. mairei E3
A. macrotera var. mairei E211
A. uniflora E48
A. chinensis var. ionandra E231
A. chinensis var. ionandra E230
A. chinensis var. ionandra E167
A. chinensis var. ionandra E30
A. chinensis var. ionandra E229
A. chinensis var. ionandra E166
A. chinensis var. ionandra E33
A. chinensis E119
A. chinensis E111
A. × grandiflora E206
A. × grandiflora E227
A. × grandiflora E159
Diabelia sanguinea E303
D. serrata E321
Kolkwitzia amabilis E9
Dipelta floribunda E55
D. floribunda E56
Linnaea borealis E14
Vesalea occidentalis E96
Eocene
Oligocene
Miocene
Pli
Ple
50
40
30
20
10
0
Ma

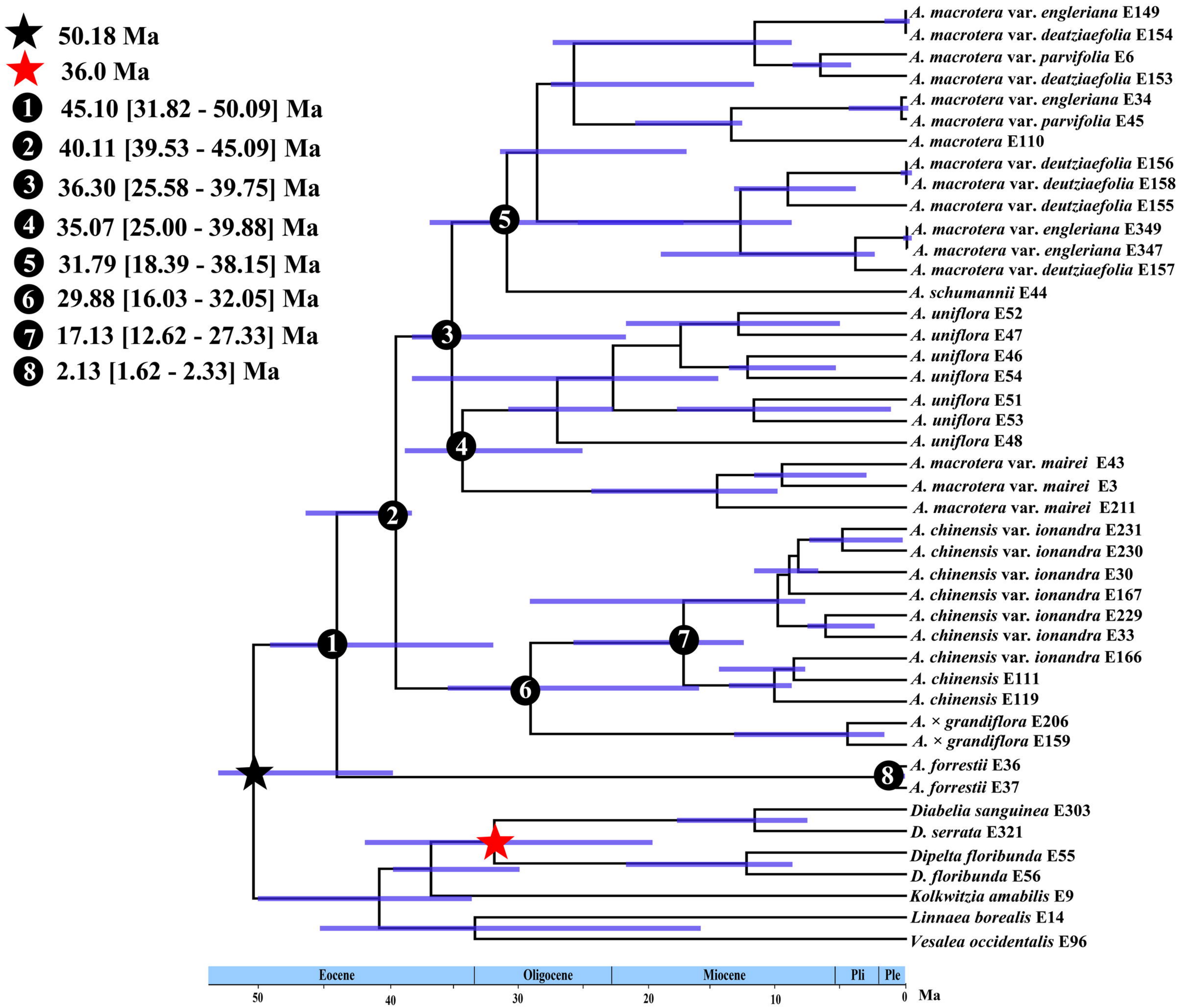
50.18 Ma
36.0 Ma
1 45.10 [31.82 - 50.09] Ma
2 40.11 [39.53 - 45.09] Ma
3 36.30 [25.58 - 39.75] Ma
4 35.07 [25.00 - 39.88] Ma
5 31.79 [18.39 - 38.15] Ma
6 29.88 [16.03 - 32.05] Ma
7 17.13 [12.62 - 27.33] Ma
8 2.13 [1.62 - 2.33] Ma
A. macrotera var. engleriana E149
A. macrotera var. deatziaefolia E154
A. macrotera var. parvifolia E6
A. macrotera var. deatziaefolia E153
A. macrotera var. engleriana E34
A. macrotera var. parvifolia E45
A. macrotera E110
A. macrotera var. deutziaefolia E156
A. macrotera var. deutziaefolia E158
A. macrotera var. deutziaefolia E155
A. macrotera var. engleriana E349
A. macrotera var. engleriana E347
A. macrotera var. deutziaefolia E157
A. schumannii E44
A. uniflora E52
A. uniflora E47
A. uniflora E46
A. uniflora E54
A. uniflora E51
A. uniflora E53
A. uniflora E48
A. macrotera var. mairei E43
A. macrotera var. mairei E3
A. macrotera var. mairei E211
A. chinensis var. ionandra E231
A. chinensis var. ionandra E230
A. chinensis var. ionandra E30
A. chinensis var. ionandra E167
A. chinensis var. ionandra E229
A. chinensis var. ionandra E33
A. chinensis var. ionandra E166
A. chinensis E111
A. chinensis E119
A. × grandiflora E206
A. × grandiflora E159
A. forrestii E36
A. forrestii E37
Diabelia sanguinea E303
D. serrata E321
Dipelta floribunda E55
D. floribunda E56
Kolkwitzia amabilis E9
Linnaea borealis E14
Vesalea occidentalis E96
Eocene
Oligocene
Miocene
Pli
Ple
50
40
30
20
10
0
Ma

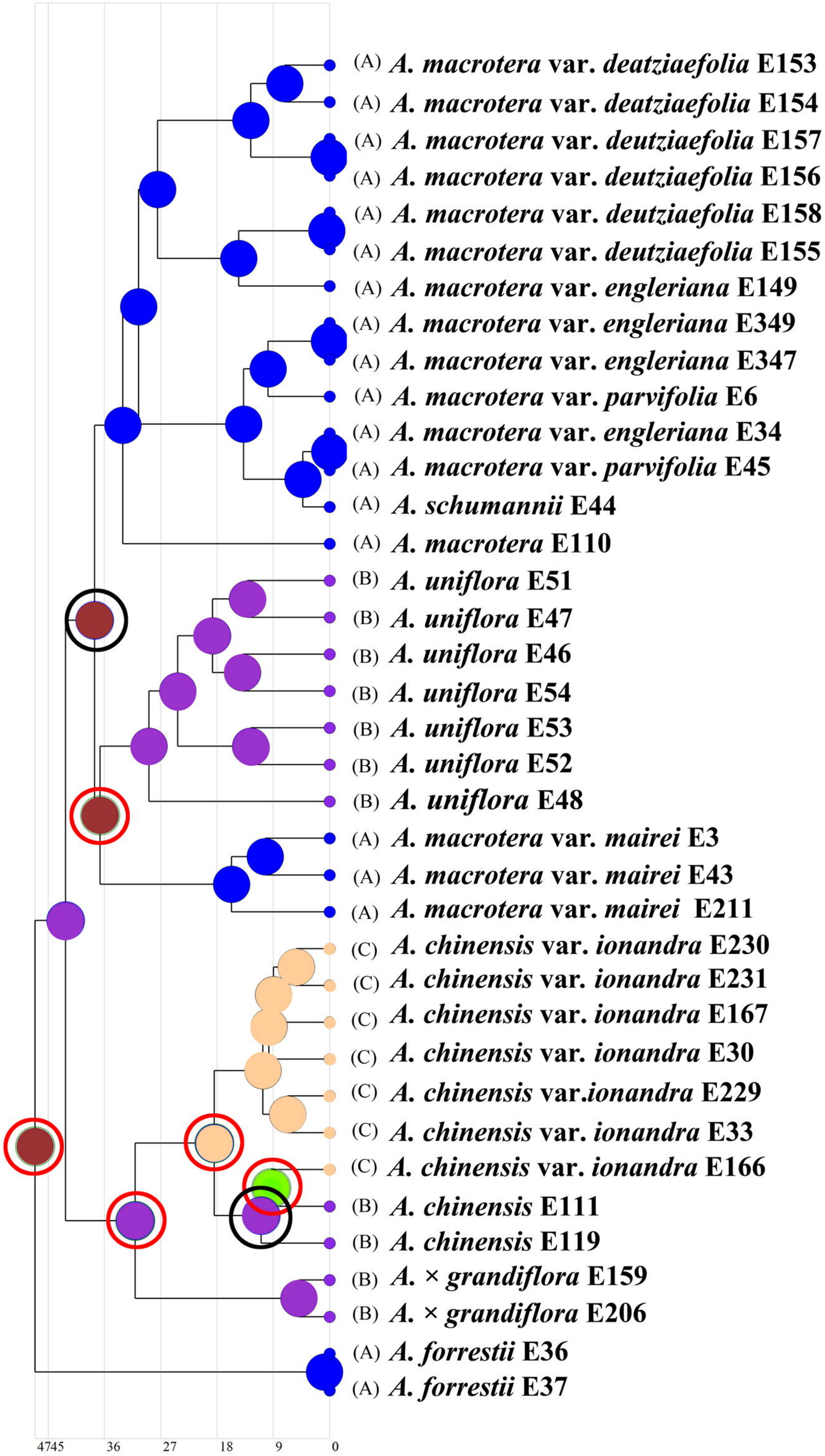
(A) A. macrotera var. deatziaefolia E153
(A) A. macrotera var. deatziaefolia E154
(A) A. macrotera var. deutziaefolia E157
(A) A. macrotera var. deutziaefolia E156
(A) A. macrotera var. deutziaefolia E158
(A) A. macrotera var. deutziaefolia E155
(A) A. macrotera var. engleriana E149
(A) A. macrotera var. engleriana E349
(A) A. macrotera var. engleriana E347
(A) A. macrotera var. parvifolia E6
(A) A. macrotera var. engleriana E34
(A) A. macrotera var. parvifolia E45
(A) A. schumannii E44
(A) A. macrotera E110
(B) A. uniflora E51
(B) A. uniflora E47
(B) A. uniflora E46
(B) A. uniflora E54
(B) A. uniflora E53
(B) A. uniflora E52
(B) A. uniflora E48
(A) A. macrotera var. mairei E3
(A) A. macrotera var. mairei E43
(A) A. macrotera var. mairei E211
(C) A. chinensis var. ionandra E230
(C) A. chinensis var. ionandra E231
(C) A. chinensis var. ionandra E167
(C) A. chinensis var. ionandra E30
(C) A. chinensis var.ionandra E229
(C) A. chinensis var. ionandra E33
(C) A. chinensis var. ionandra E166
(B) A. chinensis E111
(B) A. chinensis E119
(B) A. × grandiflora E159
(B) A. × grandiflora E206
(A) A. forrestii E36
(A) A. forrestii E37
4745
36
27
18
9
0

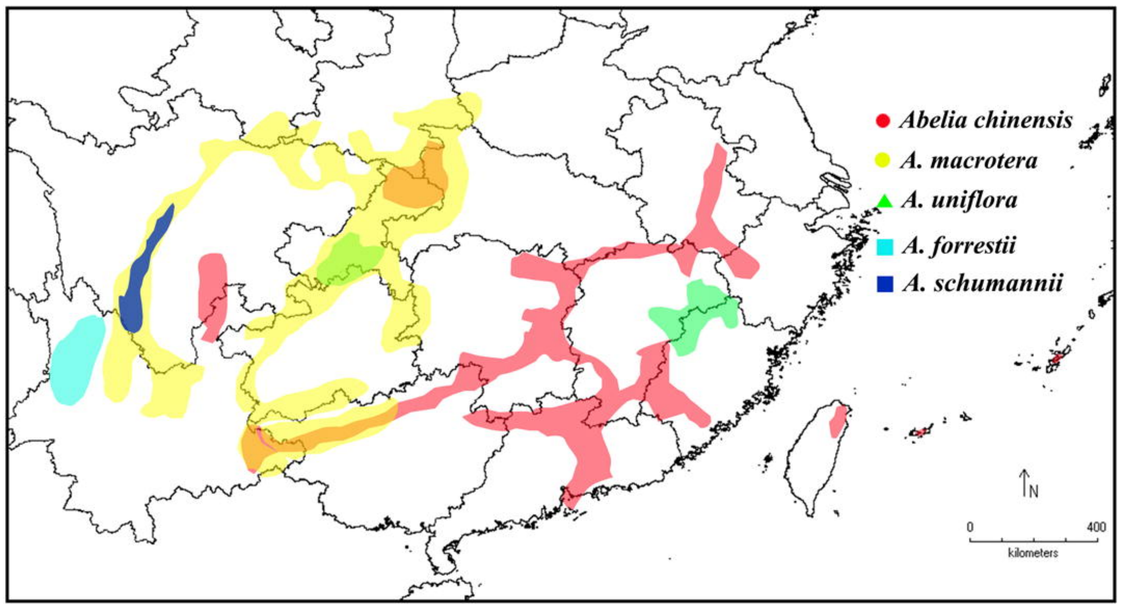
Abelia chinensis
A. macrotera
A. uniflora
A. forrestii
A. schumannii
N
0
400
kilometers

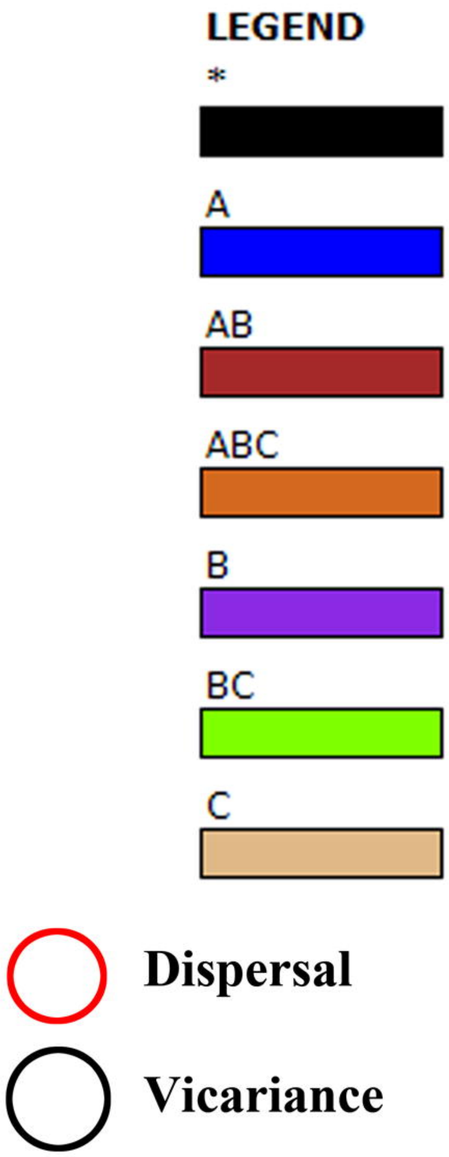
LEGEND
*
A
AB
ABC
B
BC
C
Dispersal
Vicariance

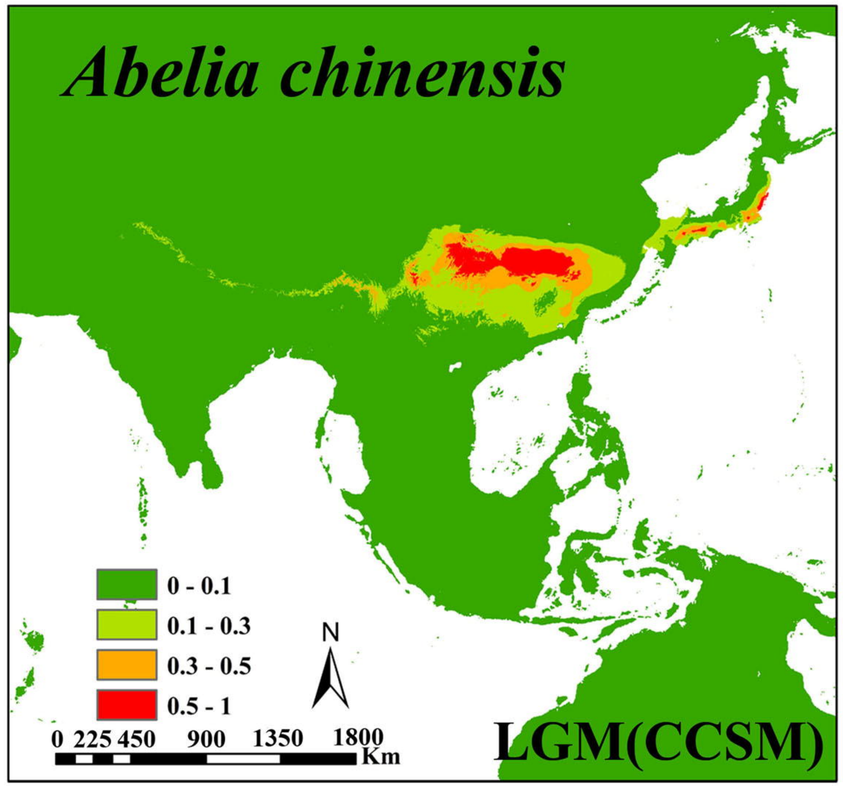
Abelia chinensis
0 - 0.1
0.1 - 0.3
0.3 - 0.5
0.5 - 1
N
0 225 450 900 1350 1800
Km
LGM(CCSM)

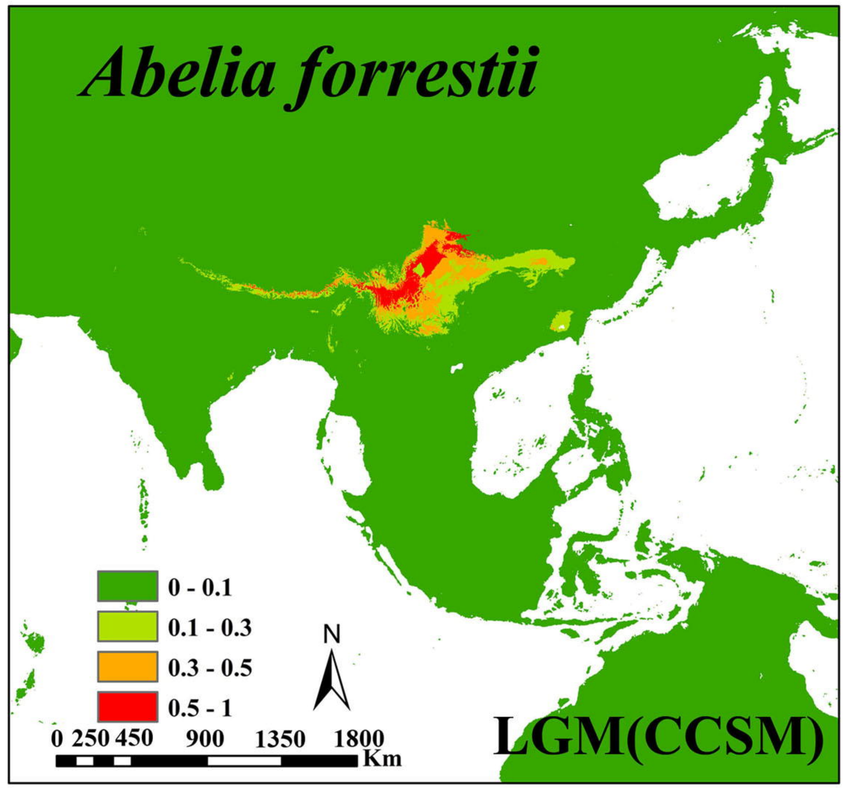
Abelia forrestii
0 - 0.1
0.1 - 0.3
0.3 - 0.5
0.5 - 1
N
0 250 450 900 1350 1800
Km
LGM(CCSM)

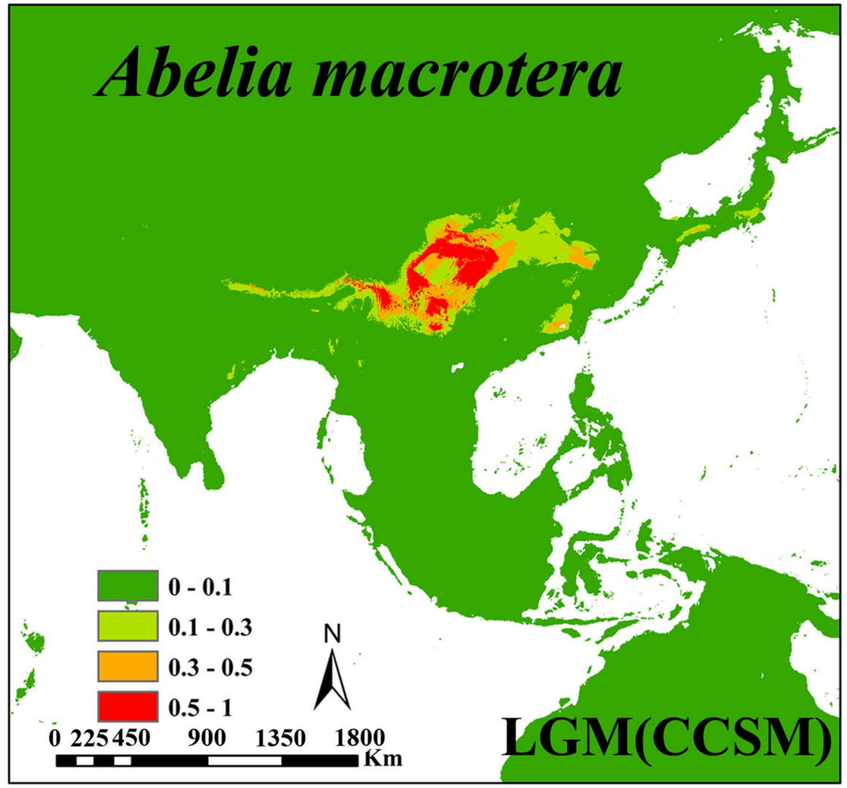
Abelia macrotera
0 - 0.1
0.1 - 0.3
0.3 - 0.5
0.5 - 1
N
0 225 450 900 1350 1800
Km
LGM(CCSM)

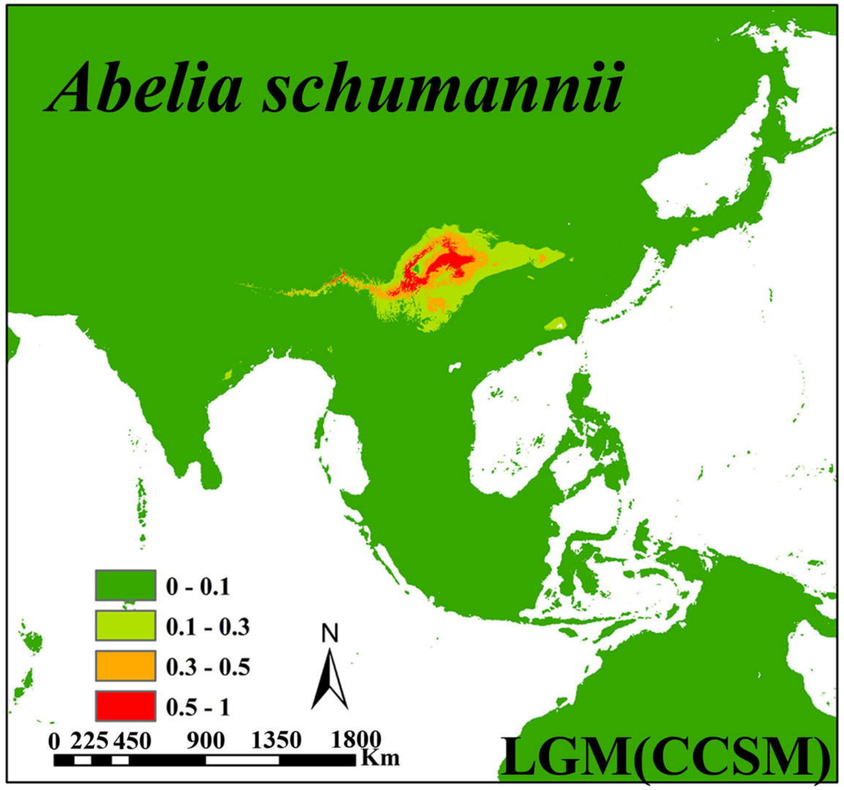
Abelia schumannii
0 - 0.1
0.1 - 0.3
0.3 - 0.5
0.5 - 1
N
0 225 450 900 1350 1800
Km
LGM(CCSM)

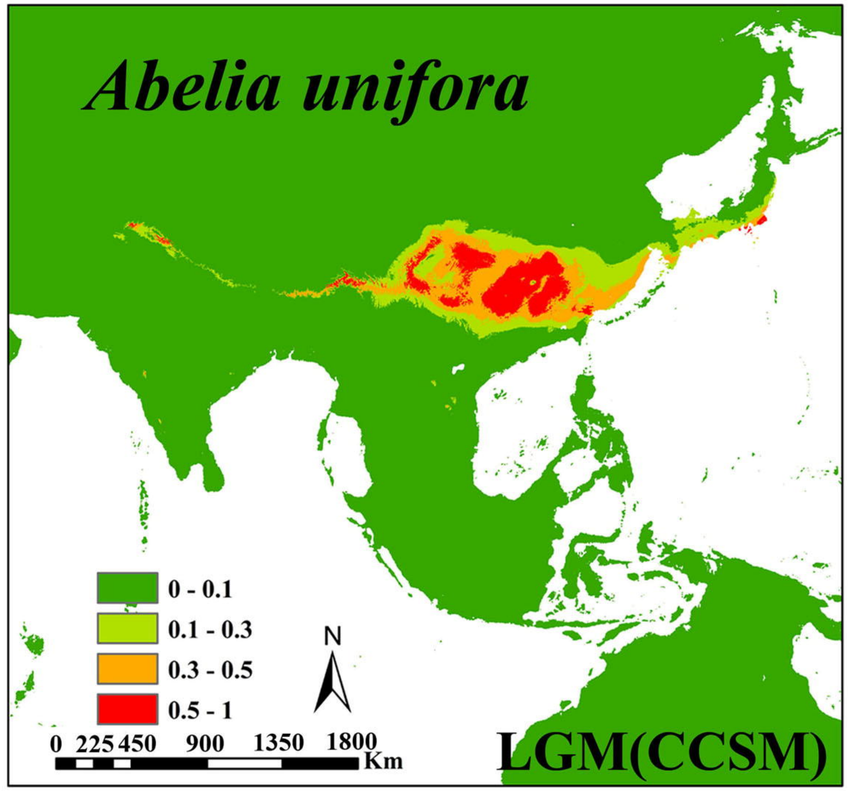
Abelia unifora
0 - 0.1
0.1 - 0.3
0.3 - 0.5
0.5 - 1
N
0 225 450 900 1350 1800
Km
LGM(CCSM)

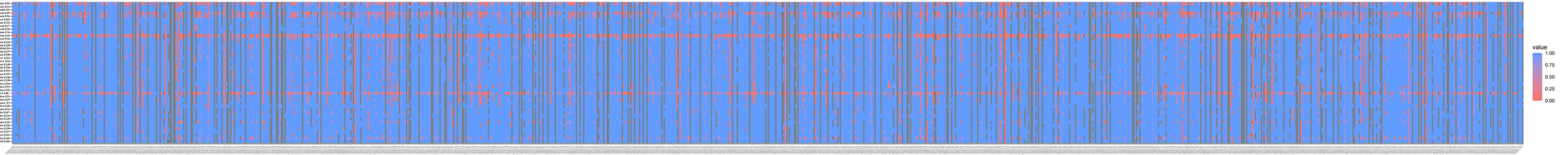
Ursalar ursolensis E96
Limnias barrulis E14
Rathvilia amabilis E9
Dipsilia flavibasis E9
D. flavibasis E96
Dinotrichia sinensis E9
D. serrata E32
A. formosi E37
A. formosi E96
A. macrotera var. purpurea E96
A. macrotera var. purpurea E48
A. schomburgkii E14
A. macrotera E110
A. macrotera var. purpurea E9
A. macrotera var. purpurea E6
A. macrotera var. dentifolia E107
A. macrotera var. motor E96
A. macrotera var. motor E21
A. macrotera var. motor E45
A. macrotera var. dentifolia E9
A. macrotera var. dentifolia E106
A. macrotera var. dentifolia E103
A. macrotera var. angustina E107
A. macrotera var. dentifolia E106
A. macrotera var. dentifolia E9
A. aniflora E94
A. aniflora E93
A. aniflora E96
A. aniflora E48
A. aniflora E92
A. aniflora E9
A. macrotera var. motor E3
A. aniflora E46
A. chikusii var. innumba E37
A. chikusii var. innumba E107
A. chikusii var. innumba E96
A. chikusii var. innumba E129
A. chikusii var. innumba E26
A. chikusii var. innumba E9
A. v. grandiflora E109
A. v. grandiflora E127
A. chikusii E101
A. chikusii var. innumba E104
A. sp. hybrid E96
value
1.00
0.75
0.50
0.25
0.00

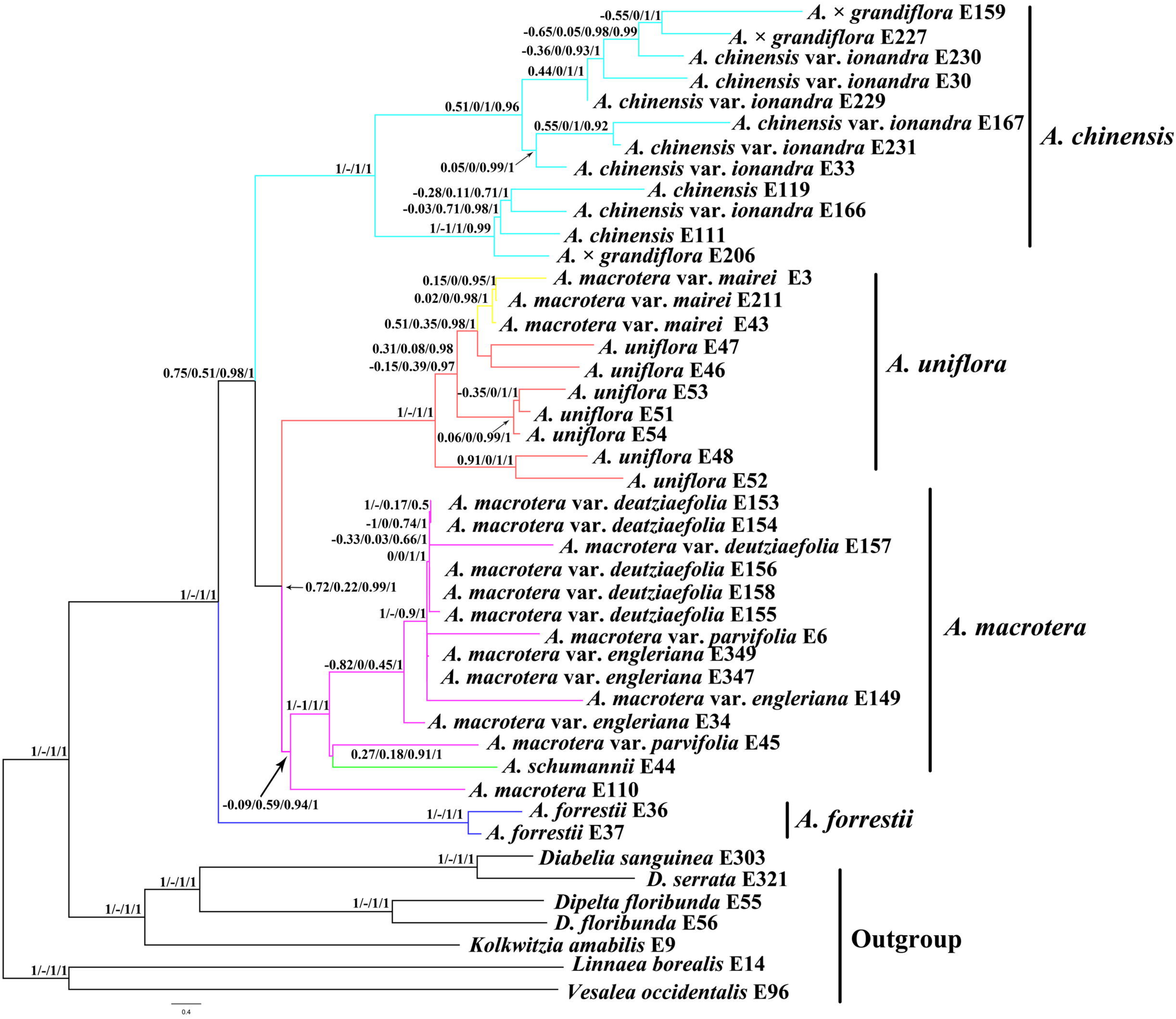
A. × grandiflora E159
A. × grandiflora E227
A. chinensis var. ionandra E230
A. chinensis var. ionandra E30
A. chinensis var. ionandra E229
A. chinensis var. ionandra E167
A. chinensis var. ionandra E231
A. chinensis var. ionandra E33
A. chinensis E119
A. chinensis var. ionandra E166
A. chinensis E111
A. × grandiflora E206
A. chinensis
A. macrotera var. mairei E3
A. macrotera var. mairei E211
A. macrotera var. mairei E43
A. uniflora E47
A. uniflora E46
A. uniflora E53
A. uniflora E51
A. uniflora E54
A. uniflora E48
A. uniflora E52
A. uniflora
A. macrotera var. deatziaefolia E153
A. macrotera var. deatziaefolia E154
A. macrotera var. deutziaefolia E157
A. macrotera var. deutziaefolia E156
A. macrotera var. deutziaefolia E158
A. macrotera var. deutziaefolia E155
A. macrotera var. parvifolia E6
A. macrotera var. engleriana E349
A. macrotera var. engleriana E347
A. macrotera var. engleriana E149
A. macrotera var. engleriana E34
A. macrotera var. parvifolia E45
A. schumannii E44
A. macrotera E110
A. macrotera
A. forrestii E36
A. forrestii E37
A. forrestii
Diabelia sanguinea E303
D. serrata E321
Dipelta floribunda E55
D. floribunda E56
Kolkwitzia amabilis E9
Linnaea borealis E14
Vesalea occidentalis E96
Outgroup
-0.55/0/1/1
-0.65/0.05/0.98/0.99
-0.36/0/0.93/1
0.44/0/1/1
0.51/0/1/0.96
0.55/0/1/0.92
0.05/0/0.99/1
1/-/1/1
-0.28/0.11/0.71/1
-0.03/0.71/0.98/1
1/-1/1/0.99
0.15/0/0.95/1
0.02/0/0.98/1
0.51/0.35/0.98/1
0.31/0.08/0.98
-0.15/0.39/0.97
0.75/0.51/0.98/1
-0.35/0/1/1
1/-/1/1
0.06/0/0.99/1
0.91/0/1/1
1/-/0.17/0.5
-1/0/0.74/1
-0.33/0.03/0.66/1
0/0/1/1
0.72/0.22/0.99/1
1/-/1/1
1/-/0.9/1
-0.82/0/0.45/1
1/-1/1/1
1/-/1/1
0.27/0.18/0.91/1
-0.09/0.59/0.94/1
1/-/1/1
1/-/1/1
1/-/1/1
1/-/1/1
1/-/1/1
1/-/1/1
0.4

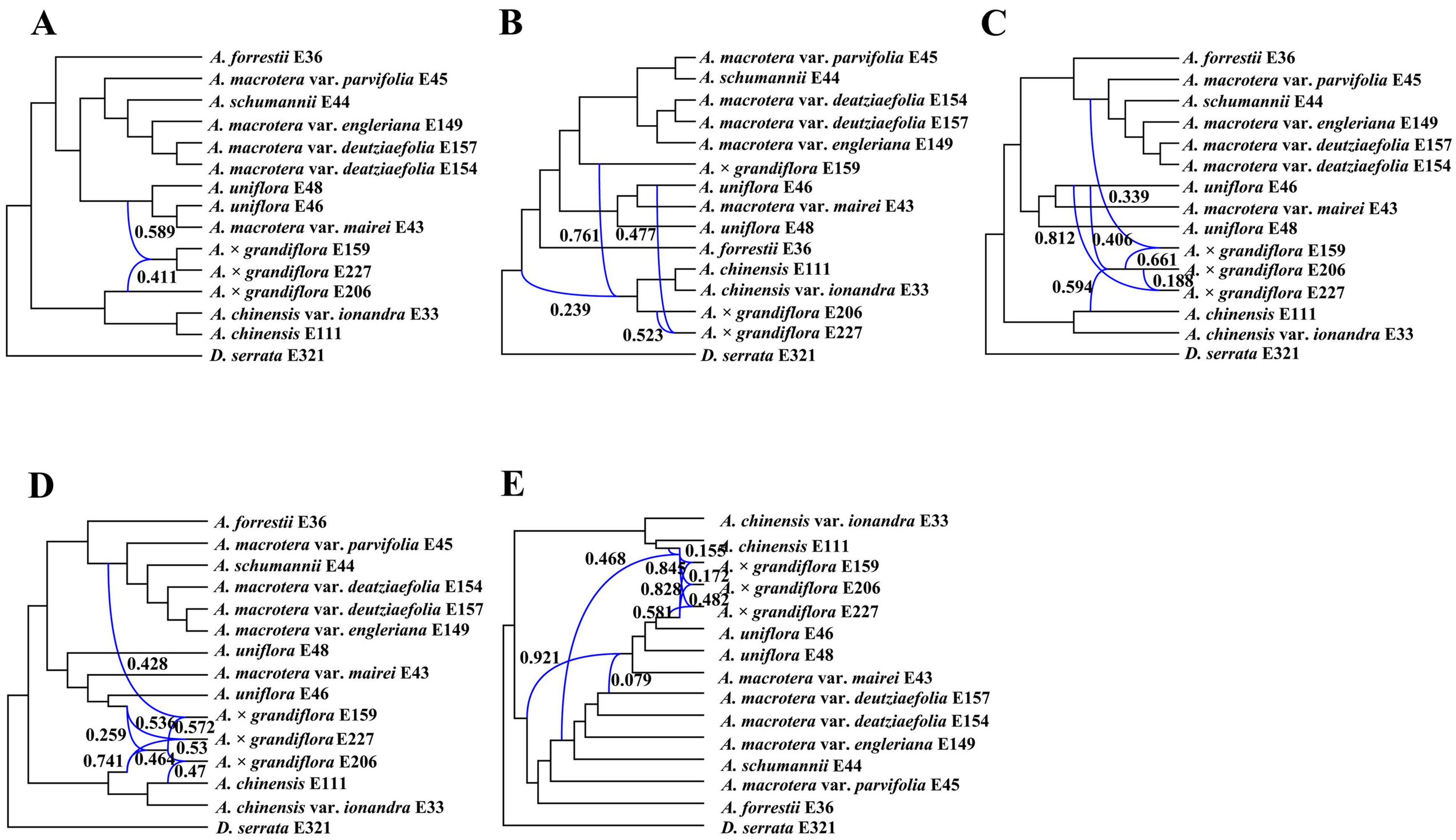
A
A. forrestii E36
A. macrotera var. parvifolia E45
A. schumannii E44
A. macrotera var. engleriana E149
A. macrotera var. deutziaefolia E157
A. macrotera var. deatziaefolia E154
A. uniflora E48
A. uniflora E46
A. macrotera var. mairei E43
A. × grandiflora E159
A. × grandiflora E227
A. × grandiflora E206
A. chinensis var. ionandra E33
A. chinensis E111
D. serrata E321
0.589
0.411
B
A. macrotera var. parvifolia E45
A. schumannii E44
A. macrotera var. deatziaefolia E154
A. macrotera var. deutziaefolia E157
A. macrotera var. engleriana E149
A. × grandiflora E159
A. uniflora E46
A. macrotera var. mairei E43
A. uniflora E48
A. forrestii E36
A. chinensis E111
A. chinensis var. ionandra E33
A. × grandiflora E206
A. × grandiflora E227
D. serrata E321
0.761
0.477
0.239
0.523
C
A. forrestii E36
A. macrotera var. parvifolia E45
A. schumannii E44
A. macrotera var. engleriana E149
A. macrotera var. deutziaefolia E157
A. macrotera var. deatziaefolia E154
A. uniflora E46
A. macrotera var. mairei E43
A. uniflora E48
A. × grandiflora E159
A. × grandiflora E206
A. × grandiflora E227
A. chinensis E111
A. chinensis var. ionandra E33
D. serrata E321
0.339
0.812
0.406
0.661
0.188
0.594
D
A. forrestii E36
A. macrotera var. parvifolia E45
A. schumannii E44
A. macrotera var. deatziaefolia E154
A. macrotera var. deutziaefolia E157
A. macrotera var. engleriana E149
A. uniflora E48
A. macrotera var. mairei E43
A. uniflora E46
A. × grandiflora E159
A. × grandiflora E227
A. × grandiflora E206
A. chinensis E111
A. chinensis var. ionandra E33
D. serrata E321
0.428
0.536
0.572
0.259
0.53
0.741
0.464
0.47
E
A. chinensis var. ionandra E33
A. chinensis E111
A. × grandiflora E159
A. × grandiflora E206
A. × grandiflora E227
A. uniflora E46
A. uniflora E48
A. macrotera var. mairei E43
A. macrotera var. deutziaefolia E157
A. macrotera var. deatziaefolia E154
A. macrotera var. engleriana E149
A. schumannii E44
A. macrotera var. parvifolia E45
A. forrestii E36
D. serrata E321
0.468
0.155
0.845
0.172
0.828
0.482
0.581
0.921
0.079

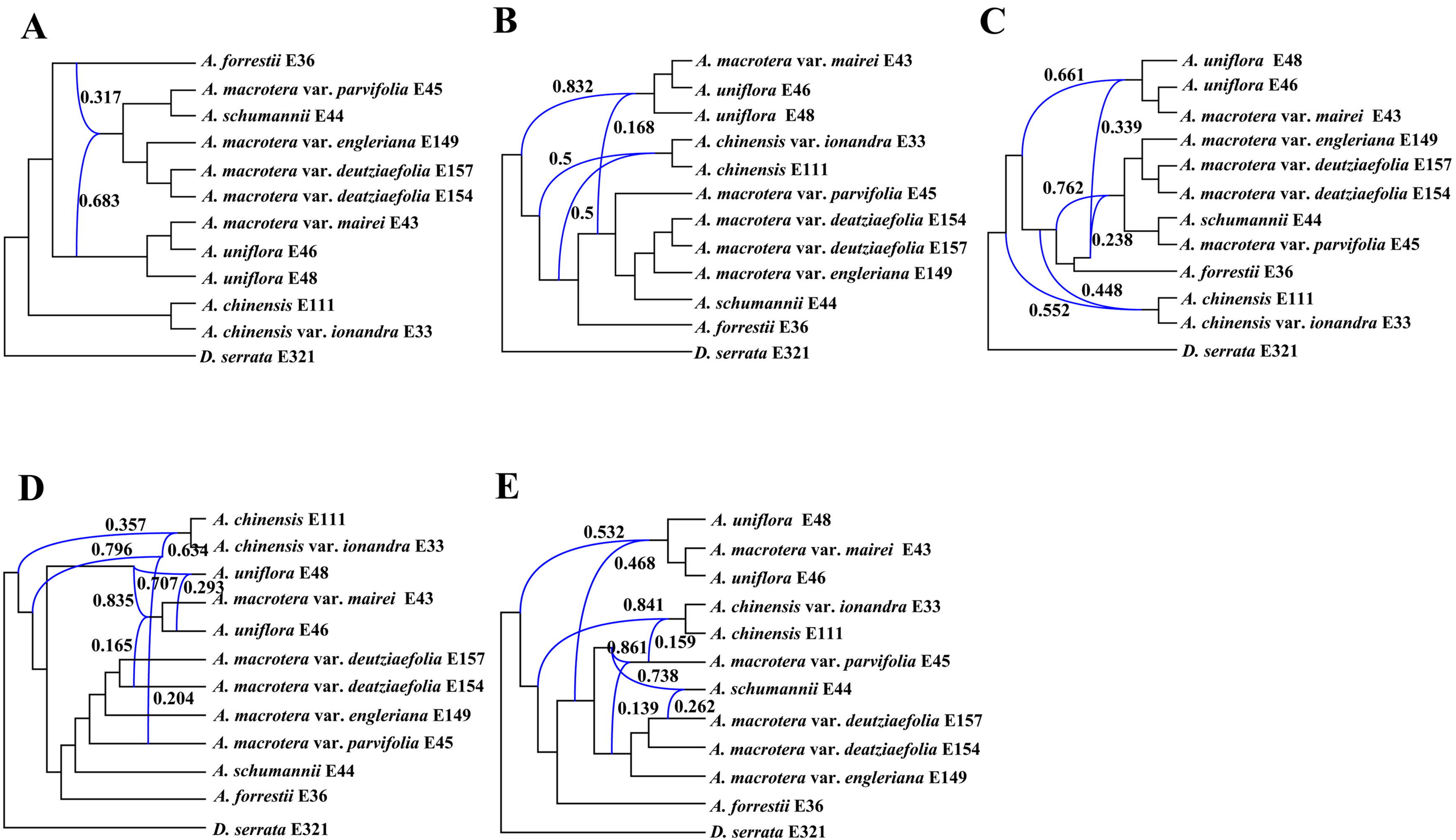
A
A. forrestii E36
A. macrotera var. parvifolia E45
A. schumannii E44
A. macrotera var. engleriana E149
A. macrotera var. deutziaefolia E157
A. macrotera var. deatziaefolia E154
A. macrotera var. mairei E43
A. uniflora E46
A. uniflora E48
A. chinensis E111
A. chinensis var. ionandra E33
D. serrata E321
0.317
0.683
B
A. macrotera var. mairei E43
A. uniflora E46
A. uniflora E48
A. chinensis var. ionandra E33
A. chinensis E111
A. macrotera var. parvifolia E45
A. macrotera var. deatziaefolia E154
A. macrotera var. deutziaefolia E157
A. macrotera var. engleriana E149
A. schumannii E44
A. forrestii E36
D. serrata E321
0.832
0.168
0.5
0.5
C
A. uniflora E48
A. uniflora E46
A. macrotera var. mairei E43
A. macrotera var. engleriana E149
A. macrotera var. deutziaefolia E157
A. macrotera var. deatziaefolia E154
A. schumannii E44
A. macrotera var. parvifolia E45
A. forrestii E36
A. chinensis E111
A. chinensis var. ionandra E33
D. serrata E321
0.661
0.339
0.762
0.238
0.448
0.552
D
A. chinensis E111
A. chinensis var. ionandra E33
A. uniflora E48
A. macrotera var. mairei E43
A. uniflora E46
A. macrotera var. deutziaefolia E157
A. macrotera var. deatziaefolia E154
A. macrotera var. engleriana E149
A. macrotera var. parvifolia E45
A. schumannii E44
A. forrestii E36
D. serrata E321
0.357
0.796
0.634
0.707
0.293
0.835
0.165
0.204
E
A. uniflora E48
A. macrotera var. mairei E43
A. uniflora E46
A. chinensis var. ionandra E33
A. chinensis E111
A. macrotera var. parvifolia E45
A. schumannii E44
A. macrotera var. deutziaefolia E157
A. macrotera var. deatziaefolia E154
A. macrotera var. engleriana E149
A. forrestii E36
D. serrata E321
0.532
0.468
0.841
0.861
0.159
0.738
0.139
0.262

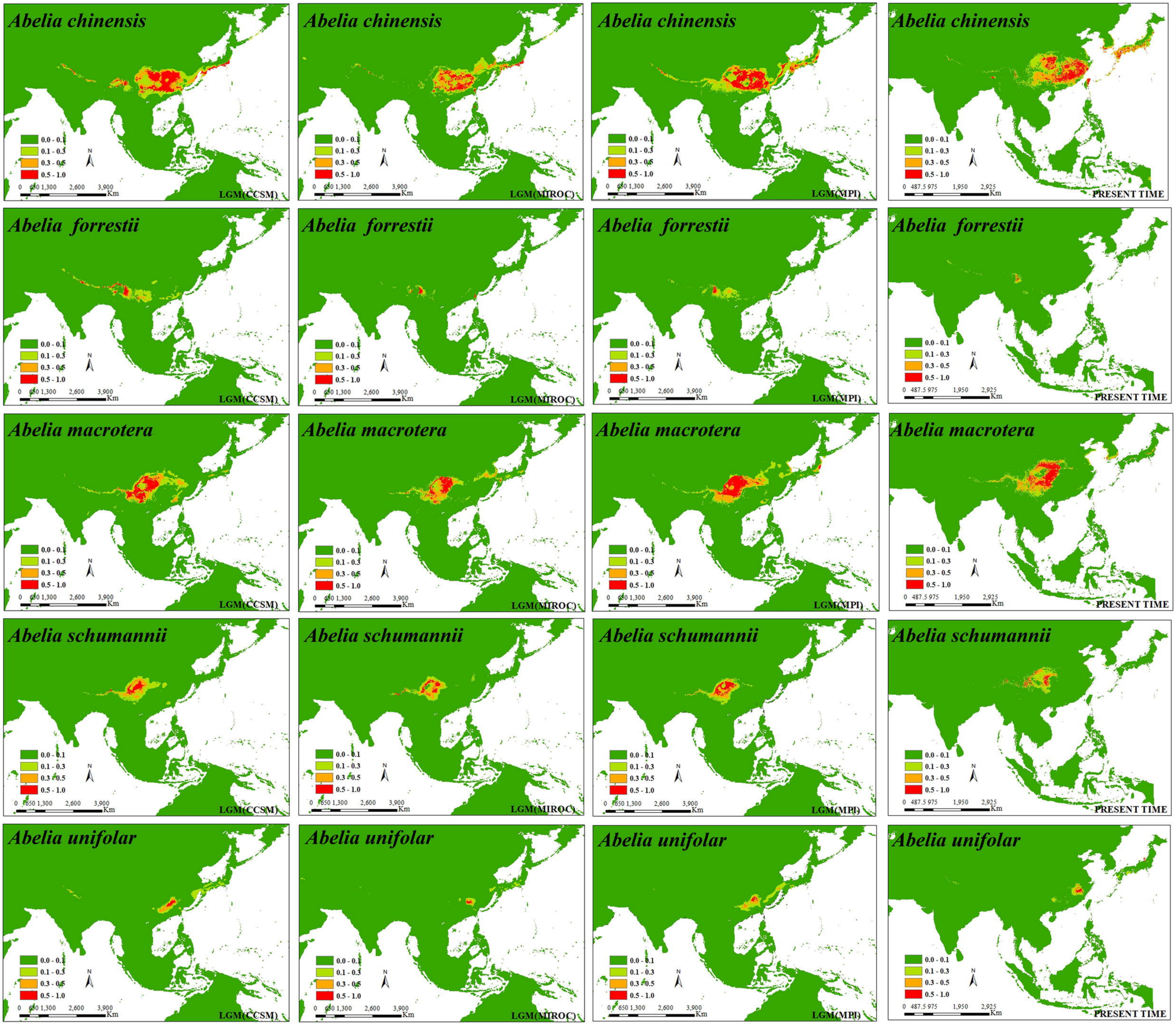
Abelia chinensis
LGM(CCSM)
Abelia chinensis
LGM(MIROC)
Abelia chinensis
LGM(MPI)
Abelia chinensis
PRESENT TIME
Abelia forrestii
LGM(CCSM)
Abelia forrestii
LGM(MIROC)
Abelia forrestii
LGM(MPI)
Abelia forrestii
PRESENT TIME
Abelia macrotera
LGM(CCSM)
Abelia macrotera
LGM(MIROC)
Abelia macrotera
LGM(MPI)
Abelia macrotera
PRESENT TIME
Abelia schumannii
LGM(CCSM)
Abelia schumannii
LGM(MIROC)
Abelia schumannii
LGM(MPI)
Abelia schumannii
PRESENT TIME
Abelia unifolar
LGM(CCSM)
Abelia unifolar
LGM(MIROC)
Abelia unifolar
LGM(MPI)
Abelia unifolar
PRESENT TIME
0.0 - 0.1
0.1 - 0.3
0.3 - 0.5
0.5 - 1.0
N
0 650 1,300 2,600 3,900 Km
0 487.5 975 1,950 2,925 Km

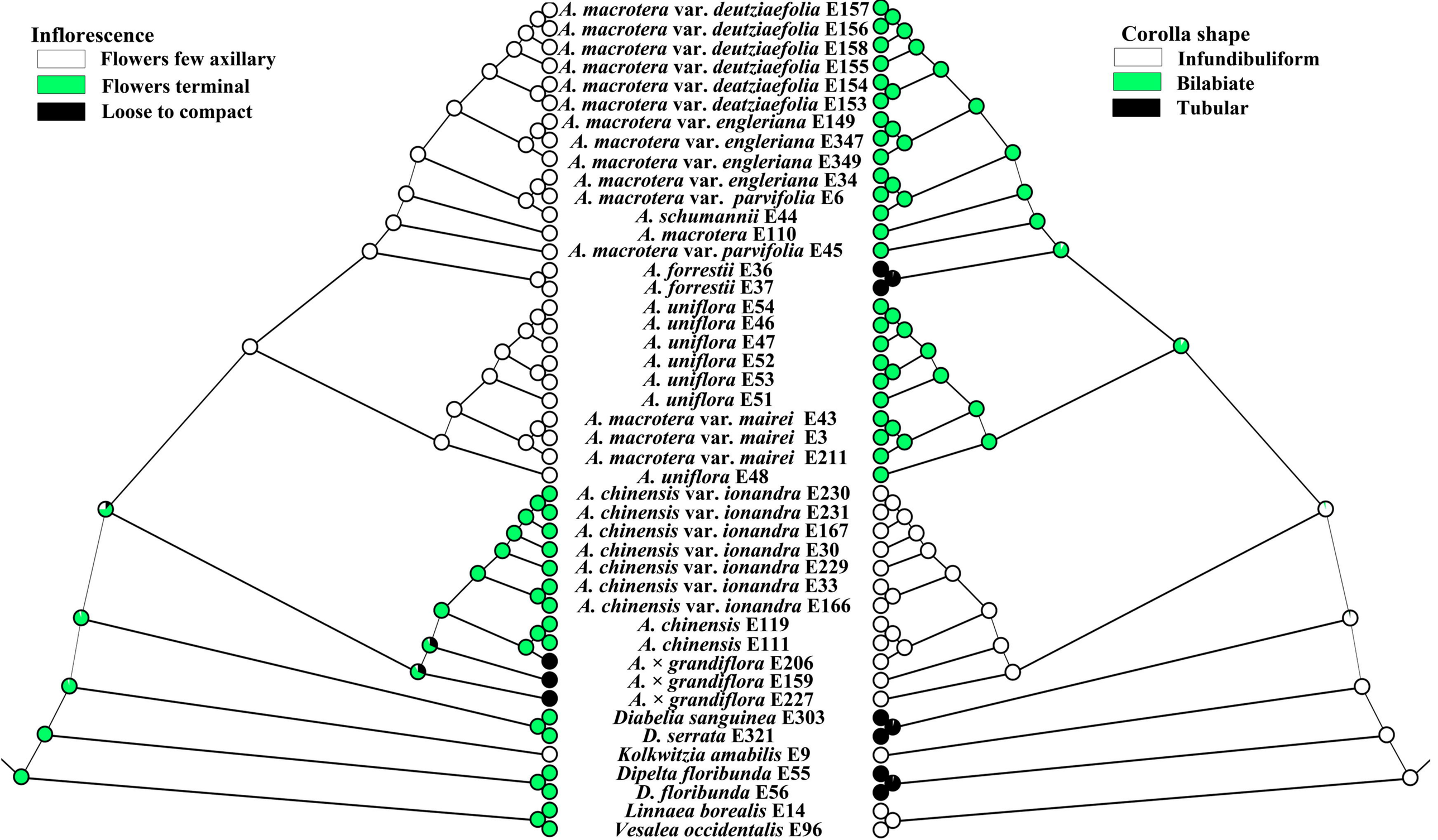
Inflorescence
Flowers few axillary
Flowers terminal
Loose to compact
Corolla shape
Infundibuliform
Bilabiate
Tubular
A. macrotera var. deutziaefolia E157
A. macrotera var. deutziaefolia E156
A. macrotera var. deutziaefolia E158
A. macrotera var. deutziaefolia E155
A. macrotera var. deatziaefolia E154
A. macrotera var. deatziaefolia E153
A. macrotera var. engleriana E149
A. macrotera var. engleriana E347
A. macrotera var. engleriana E349
A. macrotera var. engleriana E34
A. macrotera var. parvifolia E6
A. schumannii E44
A. macrotera E110
A. macrotera var. parvifolia E45
A. forrestii E36
A. forrestii E37
A. uniflora E54
A. uniflora E46
A. uniflora E47
A. uniflora E52
A. uniflora E53
A. uniflora E51
A. macrotera var. mairei E43
A. macrotera var. mairei E3
A. macrotera var. mairei E211
A. uniflora E48
A. chinensis var. ionandra E230
A. chinensis var. ionandra E231
A. chinensis var. ionandra E167
A. chinensis var. ionandra E30
A. chinensis var. ionandra E229
A. chinensis var. ionandra E33
A. chinensis var. ionandra E166
A. chinensis E119
A. chinensis E111
A. × grandiflora E206
A. × grandiflora E159
A. × grandiflora E227
Diabelia sanguinea E303
D. serrata E321
Kolkwitzia amabilis E9
Dipelta floribunda E55
D. floribunda E56
Linnaea borealis E14
Vesalea occidentalis E96

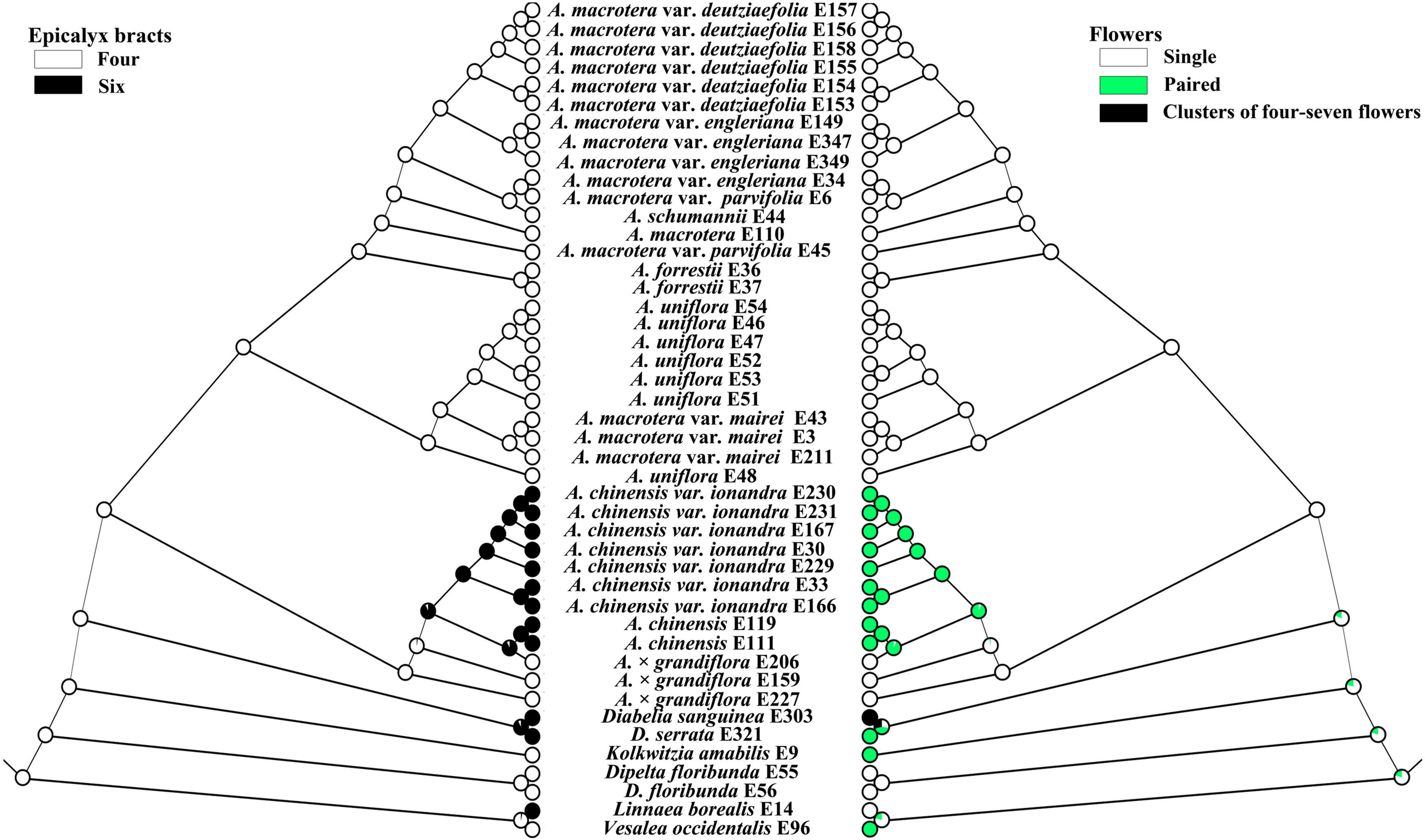
Epicalyx bracts
Four
Six
Flowers
Single
Paired
Clusters of four-seven flowers
A. macrotera var. deutziaefolia E157
A. macrotera var. deutziaefolia E156
A. macrotera var. deutziaefolia E158
A. macrotera var. deutziaefolia E155
A. macrotera var. deatziaefolia E154
A. macrotera var. deatziaefolia E153
A. macrotera var. engleriana E149
A. macrotera var. engleriana E347
A. macrotera var. engleriana E349
A. macrotera var. engleriana E34
A. macrotera var. parvifolia E6
A. schumannii E44
A. macrotera E110
A. macrotera var. parvifolia E45
A. forrestii E36
A. forrestii E37
A. uniflora E54
A. uniflora E46
A. uniflora E47
A. uniflora E52
A. uniflora E53
A. uniflora E51
A. macrotera var. mairei E43
A. macrotera var. mairei E3
A. macrotera var. mairei E211
A. uniflora E48
A. chinensis var. ionandra E230
A. chinensis var. ionandra E231
A. chinensis var. ionandra E167
A. chinensis var. ionandra E30
A. chinensis var. ionandra E229
A. chinensis var. ionandra E33
A. chinensis var. ionandra E166
A. chinensis E119
A. chinensis E111
A. × grandiflora E206
A. × grandiflora E159
A. × grandiflora E227
Diabelia sanguinea E303
D. serrata E321
Kolkwitzia amabilis E9
Dipelta floribunda E55
D. floribunda E56
Linnaea borealis E14
Vesalea occidentalis E96

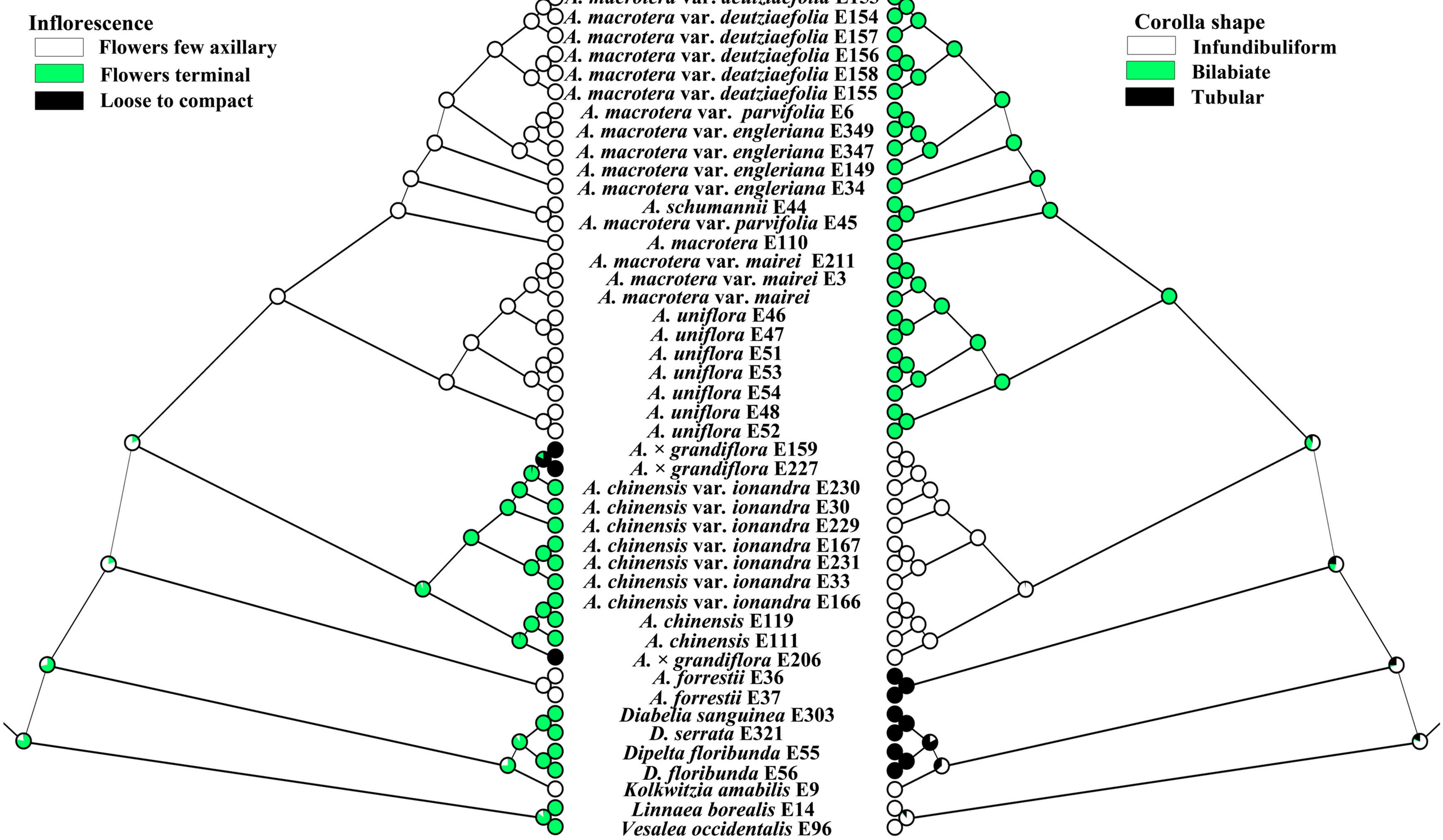
Inflorescence
Flowers few axillary
Flowers terminal
Loose to compact
Corolla shape
Infundibuliform
Bilabiate
Tubular
A. macrotera var. deutziaefolia E154
A. macrotera var. deutziaefolia E157
A. macrotera var. deutziaefolia E156
A. macrotera var. deatziaefolia E158
A. macrotera var. deatziaefolia E155
A. macrotera var. parvifolia E6
A. macrotera var. engleriana E349
A. macrotera var. engleriana E347
A. macrotera var. engleriana E149
A. macrotera var. engleriana E34
A. schumannii E44
A. macrotera var. parvifolia E45
A. macrotera E110
A. macrotera var. mairei E211
A. macrotera var. mairei E3
A. macrotera var. mairei
A. uniflora E46
A. uniflora E47
A. uniflora E51
A. uniflora E53
A. uniflora E54
A. uniflora E48
A. uniflora E52
A. × grandiflora E159
A. × grandiflora E227
A. chinensis var. ionandra E230
A. chinensis var. ionandra E30
A. chinensis var. ionandra E229
A. chinensis var. ionandra E167
A. chinensis var. ionandra E231
A. chinensis var. ionandra E33
A. chinensis var. ionandra E166
A. chinensis E119
A. chinensis E111
A. × grandiflora E206
A. forrestii E36
A. forrestii E37
Diabelia sanguinea E303
D. serrata E321
Dipelta floribunda E55
D. floribunda E56
Kolkwitzia amabilis E9
Linnaea borealis E14
Vesalea occidentalis E96

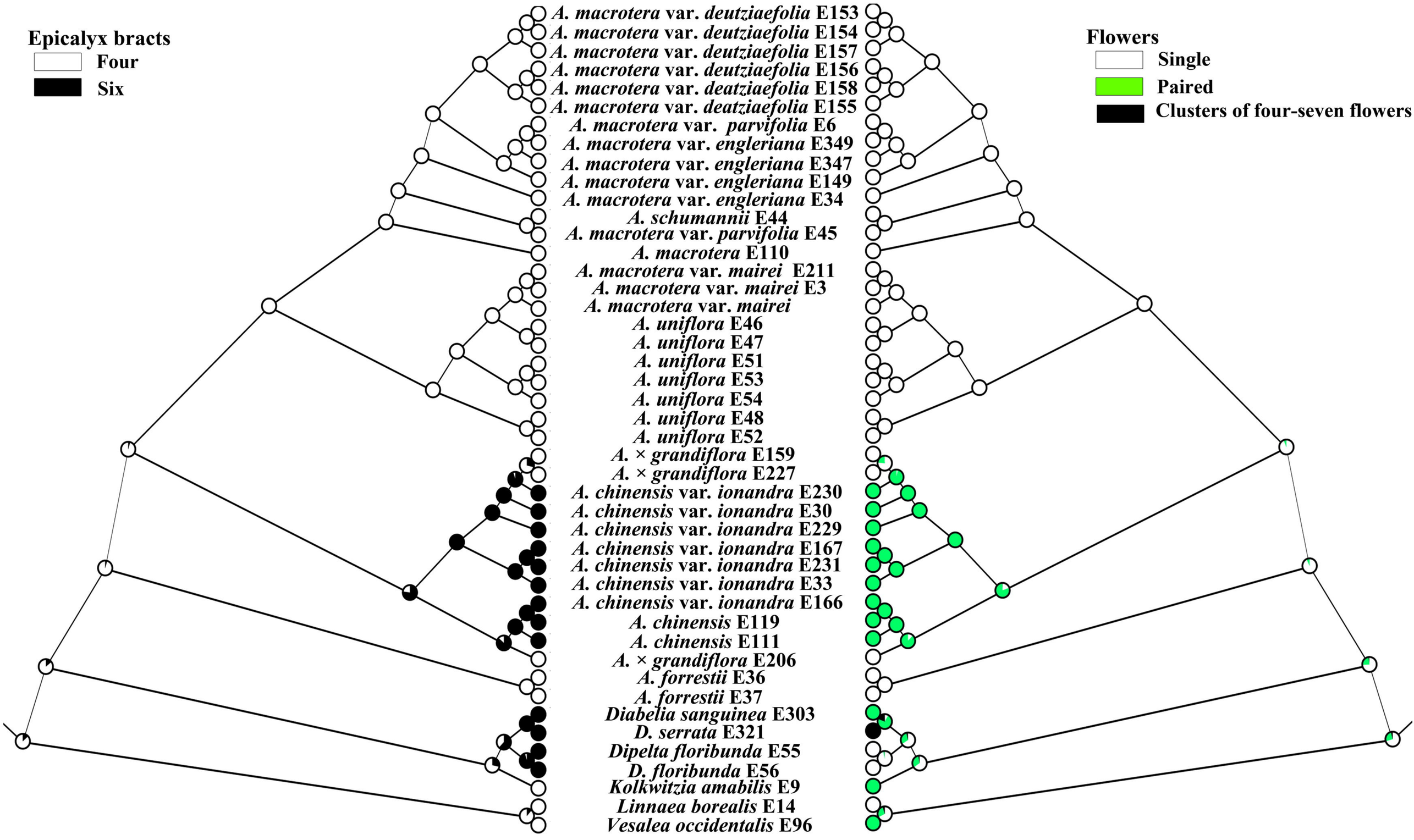
Epicalyx bracts
Four
Six
Flowers
Single
Paired
Clusters of four-seven flowers
A. macrotera var. deutziaefolia E153
A. macrotera var. deutziaefolia E154
A. macrotera var. deutziaefolia E157
A. macrotera var. deutziaefolia E156
A. macrotera var. deatziaefolia E158
A. macrotera var. deatziaefolia E155
A. macrotera var. parvifolia E6
A. macrotera var. engleriana E349
A. macrotera var. engleriana E347
A. macrotera var. engleriana E149
A. macrotera var. engleriana E34
A. schumannii E44
A. macrotera var. parvifolia E45
A. macrotera E110
A. macrotera var. mairei E211
A. macrotera var. mairei E3
A. macrotera var. mairei
A. uniflora E46
A. uniflora E47
A. uniflora E51
A. uniflora E53
A. uniflora E54
A. uniflora E48
A. uniflora E52
A. × grandiflora E159
A. × grandiflora E227
A. chinensis var. ionandra E230
A. chinensis var. ionandra E30
A. chinensis var. ionandra E229
A. chinensis var. ionandra E167
A. chinensis var. ionandra E231
A. chinensis var. ionandra E33
A. chinensis var. ionandra E166
A. chinensis E119
A. chinensis E111
A. × grandiflora E206
A. forrestii E36
A. forrestii E37
Diabelia sanguinea E303
D. serrata E321
Dipelta floribunda E55
D. floribunda E56
Kolkwitzia amabilis E9
Linnaea borealis E14
Vesalea occidentalis E96